ENHANCING THE THERAPEUTIC POTENTIAL OF HETEROCYCLIC LIGANDS FOR TREATING ALZHEIMER'S DISEASE

By

Nishanth S. Sadagopan

Submitted in partial fulfillment of the

requirements for Departmental Honors in

the Department of Chemistry & Biochemistry

Texas Christian University

Fort Worth, Texas

May 3, 2021

ENHANCING THE THERAPEUTIC POTENTIAL OF HETEROCYCLIC LIGANDS FOR TREATING ALZHEIMER'S DISEASE

Project Approved:

Supervising Professor: Kayla N. Green, Ph.D.

Department of Chemistry & Biochemistry

David Minter, Ph.D.

Department of Chemistry & Biochemistry

Matt Hale, Ph.D.

Department of Biology

Department Chair: Eric Simanek, Ph.D.

Department of Chemistry & Biochemistry

Abstract

Alzheimer's disease is a neurodegenerative disorder that is characterized by amyloid-beta plaques, neurofibrillary tangles, and unregulated reactive oxygen species. The production of reactive oxygen species in the brain is exacerbated by an excess of free-metal ions in nervous tissue. Our team and others have shown a library of tetra-azamacrocycles to have the ability to scavenge free-metal ions and quench reactive oxygen species. These macrocyclic ligands have, thus, been considered as potential therapeutic agents for combatting Alzheimer's disease. The ability of a neuro-active pharmaceutical to cross the blood-brain barrier is crucial to its pharmacological success and has proven to be a significant challenge to date in moving molecules from the bench to clinical treatment paradigms. The aim of this work is to enhance the pharmacological potential of these macrocyclic ligands. To accomplish this, computational analyses were performed on two tetra-azamacrocycles to predict their baseline blood-brain barrier permeability. The structures of these macrocycles were then modified with various moieties and analyzed via the same computational methods to predict their blood-brain barrier permeability potential. One target modification this project is focused on is the attachment of omega-3 fatty acids to these tetra-azamacrocycles. Omega-3 fatty acids have been shown to have beneficial anti-inflammatory properties *in vivo* and have the ability to assist in transporting molecules across the blood-brain barrier. Thus, the inclusion of these moieties to the structure of the Green Group ligands are attractive in regard to enhancing their pharmacological potential. To accomplish this attachment, the synthetic approach of one of the Green Group's flagship tetra-azamacrocycles, $^{OH}PyN_3$, had to be completely reimagined. New synthetic approaches and protection strategies were employed to achieve a suitable intermediate molecule primed for the addition omega-3 fatty acids. These novel synthetic methods and subsequent results are discussed in this work herein.

Acknowledgments

I would like to thank everyone who helped to make this thesis come to fruition. I would like to thank everyone in my honors committee, the Department of Chemistry and Biochemistry, the John V. Roach Honors College, the College of Science and Engineering, and everyone else who contributed to this project.

To Dr. Green, you have helped me in more ways than you could ever know. I am so grateful for how much you have helped me to become a better scientist and person over the years. You have cultivated a love of science and investigation in me and you are a big reason why I want my future medical career to center around research. I could not have made it through my undergraduate career without your guidance and your constant support. You gave me confidence when I had none, direction when I was directionless, and meaning in my work. From the bottom of my heart, thank you.

To Mom, Appa, and Nandini, thank you for always believing in me and being my support system that I know will always be there. Your love and your support has kept me going even when I didn't know where to turn to next. I know you will always love me no matter what and I will always love you all. I hope that I can make you proud as I try to help people in the world just like you taught me to. I love you all with everything I am for I am nothing without you.

To Dr. Minter, I could never have been as successful in my endeavors if it weren't for your guidance. You made every learning opportunity exciting and relevant and your teaching is the sole reason I wanted to be a synthetic chemist during my undergraduate career. It has been my absolute pleasure to have you as a mentor, a confidant, and a racquetball partner. Thank you for believing in me and supporting me without fail.

To Kristof and Sugam, you both have been the best mentors and friends I could have asked for and I couldn't imagine my research career without your constant support. If there is one thing that I know to be unequivocally true, it is that I would be nowhere as confident in my science without either of you. I hope that I was able to make you both proud as your mentee. I cannot wait to see the great work that you both produce in the future. In a million years, I could never thank you enough for putting up with me and my mistakes and my questions. I have learned so much about life and science from you both and I will be forever grateful.

To Jake and Lauren, look how far we've come. From late night study sessions in the library our Freshman year, to all the accolades you have both received as top performers in your fields, you both have done it all. Jake, I cannot wait to see you grow into the best physician the world has ever seen. Lauren, I will be reading every single paper that you publish as a synthetic chemist. In both of your quests for the stars, you have brought me with you and I am forever grateful to you both. You each have a piece of my heart and you will forever be my greatest inspirations.

To my roommates Nick, Wes, and Derek, you are my best friends and my brothers. I am not exaggerating when I say that I don't think I could have made it through these past four years without you. Through thick and thin, good times and bad times, I could always count on every single one of you. You are my best friends for life. I love you all.

Finally, to my love, my partner, my other half, Brianna, what could I even say to you that you don't know already? You are my rock and my inspiration. I want to do great things in life to make you proud. I would not be half the man I am today without you. I cannot wait for the rest of our journey together. I love you.

Table of Contents

Terminology and Abbreviations

Abbreviation	Full term
AD	Alzheimer's Disease
BBB	Blood brain barrier
clogP	Calculated logarithm of the octanol-water partition coefficient
CNS	Central nervous system
DMF	N, N-dimethylformamide
DMSO	Dimethyl sulfoxide
Et_2NH	Diethylamine
NMR	Nuclear magnetic resonance
PAMPA-BBB	Parallel artificial membrane permeability assay adapted for the blood-brain barrier
Pgp	P-glycoprotein
PSA	Polar surface area
ROS	Reactive oxygen species

List of Figures

List of Tables

List of Schemes

Introduction

I. Characteristics and pharmacological potential of tetra-azamacrocycles

Tetra-azamacrocycles are multidentate ligands that are of great interest in the field of organometallic, bioinorganic, and medicinal chemistry due to their ability to regulate free-metal ions and reactive oxygen species (ROS).[1-3] Tetra-azamacrocycles contain four heterocyclic nitrogen atoms that are capable of chelating free metal ions that can exacerbate oxidative stress in the brain. A class of macrocyclic ligands that is of interest to the Green Group contains a pyridine ring, which confers antioxidant capabilities to these pyrodinophanes making it an ideal moiety for reducing oxidative stress (**Figure 1**).

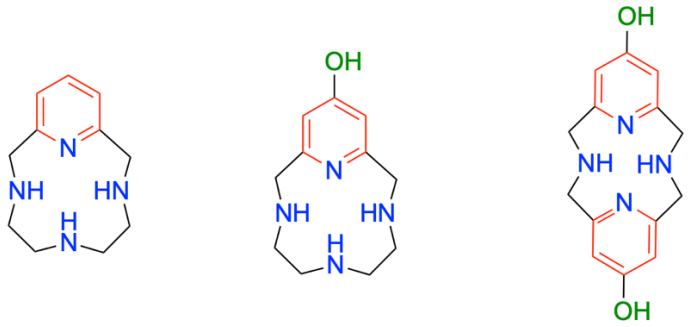

Figure 1: Green group pyridinophane library (left to right: $\mathbf{PyN_3}$, $\mathbf{^{OH}PyN_3}$, $\mathbf{^{OH}Py_2N_2}$) highlighting reactivity of each moiety (blue: metal chelating; red: antioxidant; green; radical scavenging).

This moiety is also of importance because it facilitates modification to these pyrodinophanes to further enhance the potency of these novel ligands. The synthesis and analysis of various tetra-azamacrocycles has been a focus for the Green Research Group for the past ten years.[2, 4-6] Our group and others have shown the effectiveness of these multidentate-ligands in alleviating oxidative stress in benchtop and cellular assays and have established their potential

to be used as pharmacological molecules for combatting neurodegenerative diseases such as Alzheimer's (AD).[7, 8] There are two overarching considerations that must be addressed when designing a new pharmaceutical molecule targeting the brain: the molecule must permeate through the blood-brain barrier (BBB) and retain its desired pharmacological function. Designing a molecule that satisfies both of these demands at the onset of research and development can streamline the long and laborious process of drug approval.[9-11] Tetra-azamacrocycles have been shown by this group and others to have the pharmacological potential to treat neurodegenerative diseases, but so far have not been analyzed for their ability to cross the BBB where they would be biologically active.[12] In an effort to enhance the pharmacological efficacy of these molecules, the Green Group has turned its attention towards methods of delivering these ligands to the brain.

II. Considerations for neuro-active pharmaceuticals

In order for tetra-azamacrocycles to have the desired effect of chelating free-metal ions and rebalancing levels of ROS in the brain, these ligands must have a feasible method of entry through the BBB. The BBB is maintained by epithelial cells containing gap-junctions that prevent paracellular diffusion of molecules into the brain.[13] This means that molecules must travel transcellularly through epithelial cells to gain entry through the BBB. There are a few well-established mechanisms that facilitate molecular transport across the BBB, two of which include passive diffusion and transport via P-glycoprotein (Pgp).[14] Passive diffusion is the most predominant mechanism of entry into the central nervous system (CNS) targeted by medicinal chemists.[15] This mechanism necessitates that the potential therapeutic candidate be lipophilic enough to

cross the lipid membrane of epithelial cells. As a result, in drug design there is an emphasis on the lipophilicity of the compound to optimize the ability of pharmaceuticals to permeate through lipid membranes.[16] However, because passive diffusion is a unidirectional, kinetically driven mechanism, the concentration of the dissolved potential therapeutic in the blood is important in driving the process.[17] This necessitates that the molecule in question have physical properties that facilitates its dissolution in aqueous solutions. The properties of lipophilicity and hydrophilicity are at odds with each other and, thus, require a balance that creates an optimum range of characteristics that will facilitate BBB permeation. These discordant properties pose a synthetic challenge for pharmaceutical chemists to design therapeutic molecules that fall in an optimum range that will facilitate CNS distribution. The need to identify the ideal range or combination of physical properties of a potential pharmaceutical has led to the development of parameters by which therapeutics can be analyzed for their pharmacological efficacy.

III. Analyzing ability of molecules to cross the blood-brain barrier

There are various parameters that can be used to predict the ability of a molecule to cross the BBB.[18, 19] Lipinski's Rule of Five is a well-established set of parameters that has been used to assess whether compounds are drug-like; These parameters assess the potential of these molecules to be absorbed, permeate through lipid membranes, and be pharmacologically active *in vitro*.[20, 21] For a potential pharmaceutical to satisfy Lipinski's parameters and have optimal absorption or permeation through various membranes (including the BBB), the molecule must violate as few as possible of the

following criteria: no more than five hydrogen bond donors, no more than ten hydrogen bond acceptors, a molecular weight of less than 500 daltons, and the calculated logarithm of the octanol-water partition coefficient (clogP) of no greater than five.[21, 22]

There have been many additions and variations of these criteria to more accurately predict the permeability of neuro-active drug; the polar surface area (PSA) is a measure of the area that is comprised by nitrogen and oxygen atoms in a molecule and is an indication of the extent to which a compound is hydrophilic and polar. Because PSA is tied to polarity and to hydrogen bonding capability, PSA has been used as a parameter by which to assess potential therapeutics for their ability to cross the BBB. A pharmaceutical targeting the CNS would optimally have a PSA of less than 90 $Å^2$.[23, 24] LogBB is the logarithmic ratio between concentration of a compound in the brain and in the blood.[25] LogBB is a derived from an equation that takes into account the partition coefficient and the PSA of a potential pharmaceutical. This value indicates the distribution of a molecule within the CNS and thus its ability to cross the BBB. A larger value indicates a greater ability to permeate the BBB (a value of greater than 3.0 indicates that the therapeutic candidate readily permeates the BBB, while a value of less than -1.0 indicates poor distribution in the brain).[26] An additional parameter that provides further insight into the drug-like characteristics of potential new therapeutics is the negative logarithm of the effective permeability of a compound ($–\log P_e$). This parameter is calculated by taking the logarithm of the effective permeability that is measured from a Parallel Artificial Membrane Permeability Assay adapted for the Blood Brain Barrier (PAMPA-BBB assay). A PAMPA-BBB assay serves to confirm the permeability of potential pharmaceuticals in relation to the BBB. Values of less than

5.4 indicate a high distribution in the CNS, while values of greater than 5.7 indicate poor distribution in the CNS.[27]

The Green Research Group has focused on the bioactivity of tetra-azamacrocycles but to date we have an insufficient understanding of their BBB permeability. Understanding the baseline permeability of these ligands is essential to the assessment of the efficacy of these molecules as potential neuro-active pharmaceuticals. The need for a greater understanding of the potential availability of these macrocycles in the CNS prompted further investigation into the behavior of these multi-dentate ligands. Rapid and inexpensive computational studies have been used to predict the properties of neuro-active pharmacological candidates, providing insight into the potential distribution of these candidates in the CNS.[26, 27] A similar computational analysis was performed on two tetra-azamacrocycles synthesized by the Green Group that have been shown to actively scavenge ROS and chelate free metal ions in solution, **^{OH}PyN$_3$** and **^{OH}Py$_2$N$_2$**.[7, 8] The focus of the study was to predict the likely distribution of these ligands in the brain if they were to be administered orally. The computational analysis of potential pharmaceuticals is highly dependent on molecular structure and warrants a thorough analysis of all prominent structural contributors of the molecules being assessed. Tetra-azamacrocycles are multi-dentate with multiple sites of reactivity. These sites of high electron density make them sites of protonation and deprotonation and exist in multiple forms in solution. For an accurate assessment of these ligands predicted behavior *in vivo*, they were analyzed based on the following structures: the neutral structures of these macrocycles, the structures at their reported p*I* points (the pH at which the species is neutral but contains both positively and negatively charged

moieties), and structures at physiological pH (7.4) obtained from previously reported potentiometric studies.[7, 8]

IV. Design and synthetic rationale for fatty acid-appended ligands

The Green Research Group has turned its focus towards increasing the pharmacological potential of these molecules so that they would be viable as neuro-active drugs. One method of increasing the potential of these ligands to cross the BBB is to append a fatty acid chain to the -OH moieties on the pyridinophane (**Figure 2**).

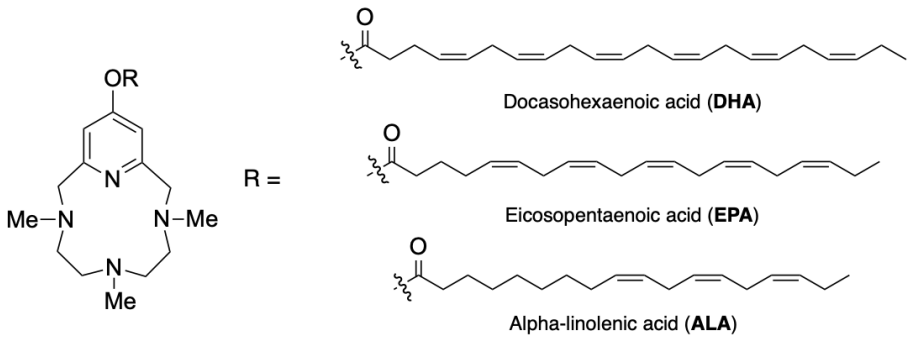

Figure 2: Proposed omega-3 acids to be appended to the pyridinophane ^{OH}**PyN**$_3$.

There is evidence to suggest that the addition of an omega-3 fatty acid chain to these ligands can increase the permeability of these ligands to the blood brain barrier, thus acting as a courier molecule for these ligands.[28, 29] In addition, omega-3 fatty acids have been shown to have beneficial anti-inflammatory properties *in vivo* and have the potential for a myriad of health benefits.[30, 31] Such an appendage has the potential to not only alleviate challenges associated with permeability, but also enhance reactivity.

There are many synthetic limitations that must be considered in conceptualizing the attachment of these fatty acids to the hydroxyl moiety of tetra-aza macrocycles. Omega-3 fatty acids are large and insoluble in aqueous solution making them difficult to be

used in synthesis. Since tetra-aza macrocycles have many reactive centers, the selection of appropriate protecting groups needs to be considered. Finally, these pyridine-containing compounds are less reactive than their benzene-containing analogues, thus, they warrant further synthetic considerations. This project is focused on the attachment of omega-3 fatty acids to one of the Green Group's flagship tetra-azamacrocycles, ^{OH}**PyN$_3$**. To accomplish this attachment, the synthetic strategy of ^{OH}**PyN$_3$** had to be completely reimagined. New synthetic approaches and protection strategies were employed to achieve a suitable intermediate primed for the addition omega-3 fatty acids. The results of these synthetic procedures are discussed in the next section. Computation was used to guide these strategies.

Results and Discussion

I. Computational Analysis of $^{OH}PyN_3$ and $^{OH}Py_2N_2$

$^{OH}PyN_3$ (Figure 3) was analyzed computationally in compliance with the previously stated parameters using Molinspiration computational software and a PAMPA-BBB assay.[32]

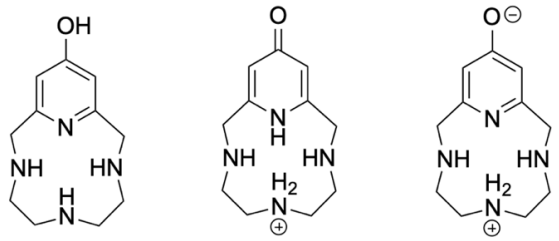

Figure 3: Three structures of **$^{OH}PyN_3$** analyzed via Lipinski computations (from left to right: drawn, physiological pH, p*I*).

Three structures of **$^{OH}PyN_3$** were analyzed via computation: its drawn structure, its structure at physiological pH (7.4), and its isoelectric point (p*I*) to gain a holistic understanding of the permeability potential of **$^{OH}PyN_3$** (**Table 1**).

Table 1: Values (MW, clog*P*, HBA, HBD, PSA, log BB) for **$^{OH}PyN_3$**.

Compound	MW	clogP	HBA	HBD	Lipinski Violations	PSA (Å)	logBB
$^{OH}PyN_3$	222.29	-0.5	5	4	0	69.2	-0.961
$^{OH}PyN_3$ at pH = 7.4	223.3	-3.36	4	4	0	73.52	-1.460
$^{OH}PyN_3$ at p*I* = 10.31	224.16	-3.1	4	4	0	76.61	-1.466
Lipinski's Rules & Other Parameters	**≤ 500**	**≤ 5.0**	**≤ 10**	**≤ 5**	**≤ 1**	**≤ 90**	**> 3.0 (readily); < -1.0 (poorly)**

The drawn structure of **$^{OH}PyN_3$** has no violations of Lipinski's general parameters but its logBB value of -0.961 indicates that **$^{OH}PyN_3$** would have a low distribution in the

CNS. If the structure of ^{OH}**PyN$_3$** at physiological pH (7.4) is assessed in the computational analysis, logBB decreases further to -1.460, which is further evidence that ^{OH}**PyN$_3$** will be poorly distributed in the brain at physiological conditions. This large decrease in logBB is attributed to the negative magnitude of the calculated partition coefficient (clogP). Protonation constants and contributing resonance structures were previously determined for ^{OH}**PyN$_3$**.[7] The results of this protonation study show that at physiological pH, ^{OH}**PyN$_3$** is charged (**Figure 3**). This vastly decreases the lipophilicity of the compound. These results were supported with data from a PAMPA-BBB assay that was conducted for ^{OH}**PyN$_3$** and ^{OH}**Py$_2$N$_2$** with three trials at increasing pH (4.5, 7.4, 10.0) with internal low and high permeable standards atenolol and propranolol HCl respectively (**Table 2**).

Table 2: PAMPA-BBB Assay Results for ^{OH}**PyN$_3$** and ^{OH}**Py$_2$N$_2$** compared with internal low and high permeable standards internal references atenolol and propranolol HCl.

Compound Name	**pH**	**Avg. P_e (10^{-6} cm/s)**	**Avg. %R[b]**	**Avg. logP_e**	**Domain, nm**
^{OH}**PyN$_3$**	4.5	< 0.05	1		250 - 350
	7.4	< 0.01	1		
	10	< 0.01	1		
^{OH}**Py$_2$N$_2$**	4.5	< 0.01	1		250 - 400
	7.4	< 0.01	3		
	10	< 0.01	2		
Atenolol	4.5	< 0.05	4		250 - 305
	7.4	< 0.05	3		
	10	< 0.05	9		
Propranolol HCl	4.5	0.49	17	-6.31	250 - 360
	7.4	25	27	-4.60	
	10	103	27	-4.03	

pH – refers to the values in donor compartment. Acceptor had a special buffer at pH = 7.4.

$\mathbf{P_e}$ – effective permeability ($x10^{-6}$ cm/sec) measured directly from assay.

pH – refers to the values in donor compartment. Acceptor had a special buffer at pH = 7.4.

%R – membrane retention.

Avg. – the value is reported as an average of triplicates.

The permeability results observed for ^{OH}**PyN$_3$** was below the detection limit in the acceptor compartment. This indicated that the results for ^{OH}**PyN$_3$** was comparable to the detection limit of low permeable standard atenolol in acceptor compartment. The average P_e of ^{OH}**PyN$_3$** could not be accurately recorded so $-\log P_e$ could not be calculated within any confidence. These results indicate that ^{OH}**PyN$_3$** would be poorly distributed in the brain if ^{OH}**PyN$_3$** were to be used as a therapeutic targeting passive transcellular transport.

Two structures of ^{OH}**Py$_2$N$_2$** were analyzed by the same parameters as ^{OH}**PyN$_3$**. The two structures that were assessed are its drawn structure and its structure at physiological pH (which is also its p*I*) (**Figure 4**).

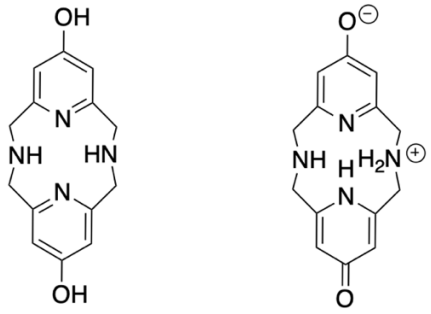

Figure 4: Two structures of ^{OH}**Py$_2$N$_2$** analyzed via Lipinski computations (from left to right: drawn and physiological pH).

As seen in **Figure 4**, at physiological pH, ^{OH}**Py$_2$N$_2$** is a zwitterion with an overall neutral charge. The dominant resonance structure for ^{OH}**Py$_2$N$_2$** at physiological pH was previously

determined via protonation study of this ligand performed by the Green Group.[8]

Table 3: Values (MW, clog*P*, HBA, HBD, PSA, log BB) for ^{OH}**Py$_2$N$_2$**.

Compound	MW	clogP	HBA	HBD	Lipinski Violations	PSA (Å)	logBB
^{OH}**Py$_2$N$_2$**	272.31	0.38	6	4	0	90.29	-1.140
^{OH}**Py$_2$N$_2$** at p*I* = 7.4	272.31	-2.37	6	4	0	97.44	-1.663
Lipinski's Rules & Other Parameters	**≤ 500**	**≤ 5.0**	**≤ 10**	**≤ 5**	**≤ 1**	**≤ 90**	**> 3.0 (readily); < -1.0 (poorly)**

The results of this study are similar to that of ^{OH}**PyN$_3$** in that they indicate that ^{OH}**Py$_2$N$_2$** would be sub-optimal in its BBB permeability potential (**Table 3**). ^{OH}**Py$_2$N$_2$** in its drawn state has no violations of Lipinski's parameters but a computed logBB of -1.140 is obtained and predicts that ^{OH}**Py$_2$N$_2$** would be poorly distributed in the brain. If the structure of ^{OH}**Py$_2$N$_2$** at physiological pH is analyzed, the value of logBB decreases further to -1.663. These results were again confirmed by the results of a PAMPA-BBB assay **(Table 2**); similar to ^{OH}**PyN$_3$**, the permeability results observed for ^{OH}**Py$_2$N$_2$** was below the detection limit in the acceptor compartment. The results of the PAMPA-BBB assay for ^{OH}**Py$_2$N$_2$** indicate a poor potential of ^{OH}**Py$_2$N$_2$** to cross the BBB. *These data indicated the need to modify the structure of these potential pharmacological macrocycles in order to enhance the pharmokinetic properties of these ligands*. Lipophilic, non-polar molecules have easy access through phospholipid bilayers as there is a direct relationship between lipophilicity and octanol-water partition coefficient. Thus, it is our hypothesis that we can enhance the pharmokinetic properties of these novel ligands by tethering permeability-enhancing, lipophilic molecules to these pyrodinophanes. The appendage of lipophilic molecules to the hydroxyl moiety of ^{OH}**PyN$_3$** is the focus of this work.

II. Computational analysis of fatty acid appended $^{OH}PyN_3$

To assess the potential benefit of appending omega-3 fatty acids to the pyridoxal function of the macrocycle $^{OH}PyN_3$, a follow-up computational study of $^{OH}PyN_3$ appended by various omega-3 fatty acids (**DHA, EPA, and ALA**) was conducted via the previously stated parameters (**Table 4**).

Table 4: Values (MW, clog*P*, HBA, HBD, PSA, log BB) for $^{OH}PyN_3$ with omega-3 fatty acid appendages (**DHA**, **EPA**, **ALA**).

Compound	MW	clogP	HBA	HBD	Lipinski Violations	PSA (Å)	logBB
$^{OH}PyN_3$ with **DHA**	532.77	5.44	6	3	2	75.28	-0.148
$^{OH}PyN_3$ with **EPA**	506.74	5.16	6	3	2	75.28	-0.191
$^{OH}PyN_3$ with **ALA**	482.71	5.6	6	3	1	75.28	-0.124
Lipinski's Rules & Other Parameters	**≤ 500**	**≤ 5.0**	**≤ 10**	**≤ 5**	**≤ 1**	**≤ 90**	**> 3.0 (readily); < -1.0 (poorly)**

As seen in **Table 4**, clogP increased drastically for all of the proposed fatty acid-appended $^{OH}PyN_3$ molecules in comparison to unaided $^{OH}PyN_3$. As a direct consequence of the increase in the value for clogP, the values of logBB also increased. While the values for logBB are still negative, the positive shift in comparison to unaided $^{OH}PyN_3$ marks improvement in the BBB permeability potential by an entire order of magnitude. While these data need to be supported by a follow-up PAMPA-BBB study, these results are promising. However, there are further considerations to be made: as the length of the fatty acid increased, the MW and clogP increased past the optimal range of orally administered, neuro-active drugs which would inhibit the ligand from

being compatible with the aqueous phase. The results of this study support the hypothesis that appending a fatty acid chain to the macrocycles could increase the potential of these ligands to cross the BBB. To accomplish this attachment, the synthetic approach of, ^{OH}**PyN$_3$**, had to be completely reimagined. New synthetic approaches and protection strategies were employed to achieve a suitable intermediate molecule primed for the addition omega-3 fatty acids.

III. Model for fatty acid appendage

A model reaction was performed to test the feasibility of esterifying a pyridinophane where the hydroxyl moiety is positioned *para* to the pyridine nitrogen (**Scheme 1**). Diethyl chelidamate was used as a model for the pyridinophane of ^{OH}**PyN$_3$** because of its facile solubility in dichloromethane and –OH group being the only potential participant in esterification (**Scheme 1**).

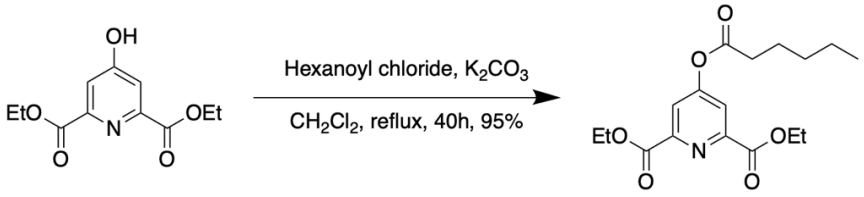

Scheme 1: Model for fatty acid attachment synthetic scheme.

Commercially available hexanoyl chloride was used as a proxy for a fatty acid because of its lipophilic hydrocarbon chain and greater reactivity as compared to hexanoic acid. The high-yielding (95%) attachment of hexanoyl chloride to the diethyl chelidamate was confirmed via NMR and indicated that ester linkages could be made to pyridoxal functionalities. The successful model for of ester appendages served as the synthetic basis for the investigation of fatty acid attachment to ^{OH}**PyN$_3$**.

IV. SES protection synthetic route

The attachment of a fatty acid molecule to the hydroxyl moiety of $^{OH}PyN_3$ required a change in the synthetic strategy for this pyrodinophane. This required utilizing a retrosynthetic approach to determine suitable protecting groups and intermediates in the synthesis of $^{OH}PyN_3$ appended with a fatty acid (**Figure 5**).

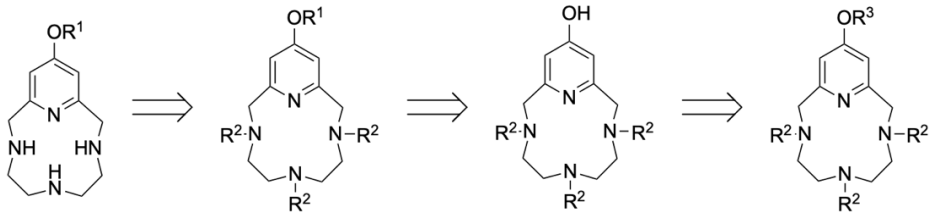

Figure 5: Retrosynthetic strategy for the synthesis $^{OH}PyN_3$ appended with an omega-3 fatty acid where R^1 is an omega-3 fatty acid, R^2 is the nitrogen protecting group, and R^3 is the pyridoxal protecting group.

As seen in **Figure 5**, R^3 must be compatible with ligand cyclization and nitrogen protection; R^2 must also be compatible with ligand cyclization, pyridoxal deprotection, and fatty acid attachment. The protecting group for the pyridoxal –OH group was chosen to be tetrahydropyran (THP). 2-(trimethylsilyl)ethanesulfonyl (or SES) was chosen to be the protecting group for the bottom functionality. The following convergent synthetic scheme was proposed to achieve the target molecule appended with an omega-3 fatty (**Scheme 2**). The results of this synthetic route proved to be challenging to overcome. As seen in **Scheme 2**, the intermediates 1-11 were obtained in good yield and purity indicating a successful synthetic route towards the target molecule. However, there were multiple difficulties in the synthetic steps in this pathway. The conversion of the fatty acid, **DHA**, to **DHA-Cl** via thionyl chloride proved to be unsuccessful as the reaction resulted starting material in the largest concentration

indicating an incomplete conversion of **DHA** to **DHA-Cl**. This led to difficulties in the next step in the attachment of **DHA** to the SES protected macrocycle.

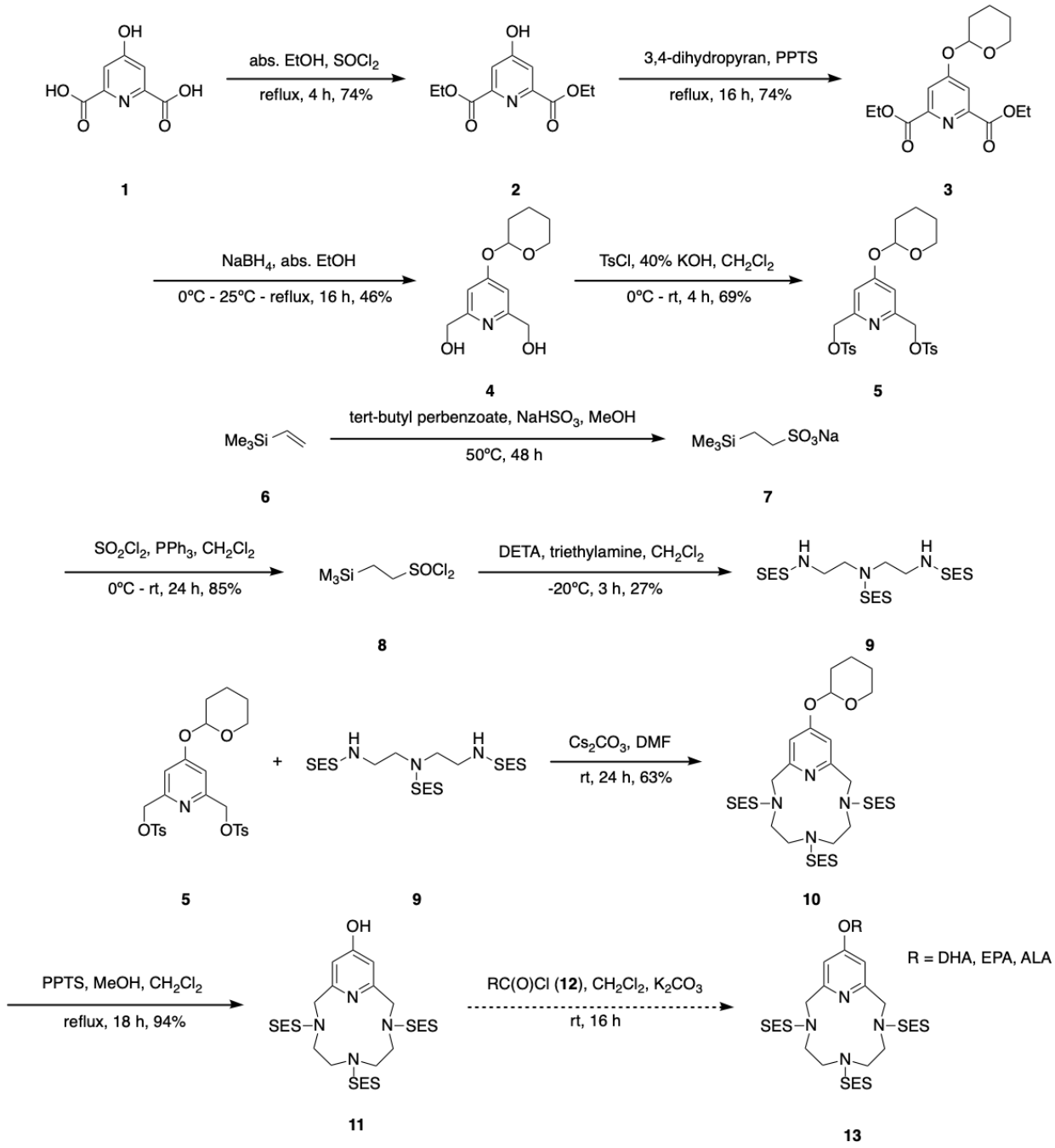

Scheme 2: Convergent synthesis of fatty acid appended ^{OH}**PyN$_3$** utilizing THP and SES protecting groups.

In addition, the deprotection of the SES protecting groups from the three aza centers was unsuccessful leading to decomposed macrocycle or partially protected macrocycle. The complications with deprotection of the SES macrocycle were too significant to overcome and required that a different synthetic route be employed. The results of this synthetic approach required that we rework our synthetic strategy and alter the structure of the target molecule. A new synthetic approach required a protecting group other than the SES protecting groups and was conducive to the attachment of a fatty acid in an ester linkage with the pyridoxal moiety.

V. Computational analysis of fatty acid-appended ^{OH}PyNMe$_3$

The difficulties of the SES protection route necessitated a change to the target molecule. In addition, the results of the computational analysis of unaided ^{OH}**PyN$_3$** indicated the need to increase the clogP of ^{OH}**PyN$_3$** to improve its BBB permeability potential. While the low partition coefficient of unaided ^{OH}**PyN$_3$** is one of the parameters that contributed to the low values of logBB for ^{OH}**PyN$_3$**, the high PSA of ^{OH}**PyN$_3$** (due to its four amino groups and one hydroxyl moiety) was also a problematic component of the calculation. A new target molecule was proposed to increase the BBB permeability potential of our target molecule as well as overcome the synthetic difficulties of the SES protection route. To both protect the four aza moieties of ^{OH}**PyN$_3$** as well as decrease its PSA and hydrogen bond donating capabilities, a methylated ^{OH}**PyN$_3$**, ^{OH}**PyNMe$_3$**, was proposed to be used for the attachment of an omega-3 fatty acid. To assess the potential benefit of appending omega-3 fatty acids to the pyridoxal function of ^{OH}**PyNMe$_3$**, a similar computational study of ^{OH}**PyNMe$_3$** appended by various omega-3 fatty acids (**DHA, EPA, and ALA**) was conducted via the previously stated parameters (**Table 5**).

Table 5: Values (MW, clog*P*, HBA, HBD, PSA, log BB) for ^{OH}**PyNMe$_3$** with omega-3 fatty acid appendages (**DHA**, **EPA**, **ALA**).

Compound	MW	clogP	HBA	HBD	Lipinski Violations	PSA (Å)	logBB
^{OH}**PyNMe$_3$** with **DHA**	574.42	7.44	6	0	2	48.38	0.554
^{OH}**PyNMe$_3$** with **EPA**	548.82	6.92	6	0	2	48.38	0.475
^{OH}**PyNMe$_3$** with **ALA**	524.41	6.73	6	0	2	48.38	0.446
Lipinski's Rules & Other Parameters	**≤ 500**	**≤ 5.0**	**≤ 10**	**≤ 5**	**≤ 1**	**≤ 90**	**> 3.0 (readily); < -1.0 (poorly)**

As seen in **Table 5**, clogP increased drastically for all of the proposed fatty acid-appended **^{OH}PyNMe$_3$** molecules in comparison to unappended, unmethylated **^{OH}PyN$_3$**. As a direct consequence of the increase in the value for clogP, the values of logBB also increased. In contrast to the proposed fatty acid appended **^{OH}PyN$_3$** molecules, the logBB of the fatty acid appended **^{OH}PyNMe$_3$** molecules increased to positive values. This indicates an even greater increase in the permeability potential of these target molecules in comparison to the previously proposed library. The positive values of logBB indicate that the new proposed library of fatty acid appended ligands have the potential to cross the BBB. While these data need to be supported by a follow-up PAMPA-BBB assay, the results are a promising and warrant a second change to our synthetic approach. The results of the synthesis of the fatty acid appended **^{OH}PyNMe$_3$** are discussed further in this work.

VI. Fatty acid-appended ^{OH}PyNMe$_3$ synthesis

The synthetic results of the SES protection route guided the methods for the synthetic pathway of **^{OH}PyNMe$_3$** and the subsequent attachment of the omega-3 fatty acid, **DHA**. The successful synthetic procedures for the top portion of the macrocycle (intermediates 1 – 5) from the SES protection route allowed for those same procedures to be used in the synthetic strategy of **^{OH}PyNMe$_3$** (**Scheme 2**). However, due to the unsuccessful deprotection attempts of the SES from the 3 aza centers in the macrocycle, a new different protection strategy had to be utilized for **1,4,7-triazaheptane** in preparation for cyclization. **2-nitrobenzenesulfonyl** (Ns) groups were chosen to be the method of protection for the 3 aza centers of **1,4,7-triazaheptane** via a modified procedure based on the work of Nicak *et al*. and used successfully by the Green group for cyclization strategies (**Scheme 3**).[33]

As seen in **Scheme 3**, after the successful cyclization leading to the THP, Ns protected ^{OH}**PyN$_3$**, the macrocycle was deprotected utilizing a one-step reaction that resulted in ^{OH}**PyN$_3$·3HCl** containing inorganic salts. ^{OH}**PyN$_3$·3HCl** could then be utilized for a methylation reaction utilizing the Eischweiler-Clarke mechanism which leads to methylation only at the nitrogen centers of the macrocycle. This prevents the possibility of methylation occurring at the free hydroxyl group. The successful Eischweiler-Clarke reaction led to the formation of ^{OH}**PyNMe$_3$** which was further purified with cold isopropanol washes to remove sodium formate salts, followed by an extraction with CH_2Cl_2 to yield the clean methylated macrocycle.

The attachment of the **DHA** to the methylated macrocycle was then attempted as the nitrogens were protected and the only possible reacting center would be the pyridine –OH. The synthesis of docosahexaenoyl chloride was based on a modified procedure proposed by Kamenecka *et al*.[34] This group had shown in the past that it was possible to convert a fatty acid such as **DHA** to the corresponding chloride which could then be used immediately to make a amide. In this particular method, we sought to use this method to make a covalent ester linkage with the pyridoxal moiety on ^{OH}**PyNMe$_3$**.

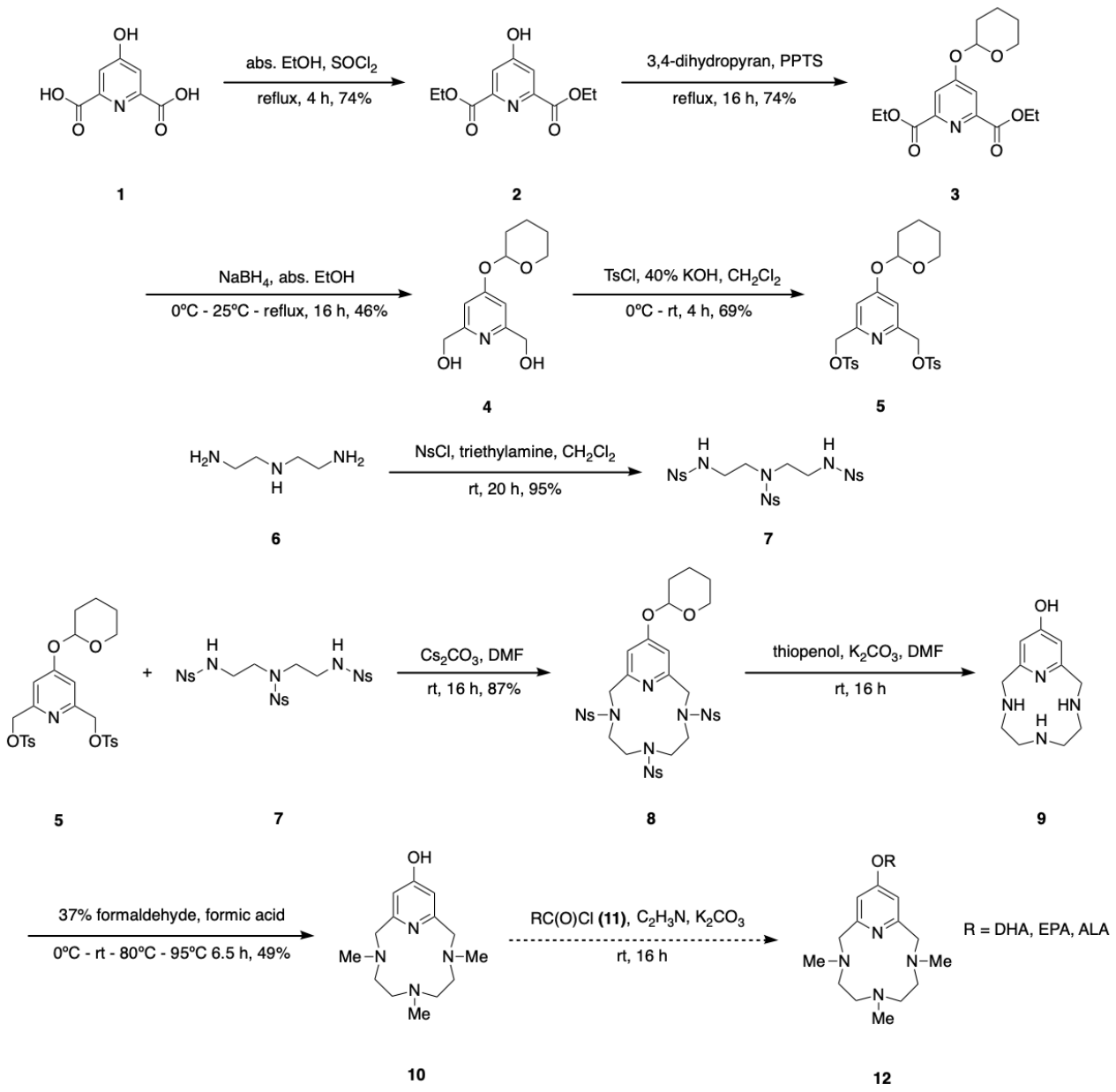

Scheme 3: Convergent synthesis for fatty acid appended ^{OH}**PyNMe3** utilizing THP and Ns protecting groups.

The crude **DHA-Cl** was immediately used to react with ^{OH}**PyNMe3** to generate the **DHA** appended ^{OH}**PyNMe3**. This reaction was conducted in acetonitrile overnight to yield a crude oil. The crude mixture was concentrated and purified with extraction with CH_2Cl_2. Upon

examination of the NMR of the concentrated organic phase, it was determined that there was no **^{OH}PyNMe$_3$** in resulting crude oil. The **^{OH}PyNMe$_3$** remained in the aqueous layer after the extraction with no fatty acid appendage. The failure to isolate of **DHA** appended **^{OH}PyNMe$_3$** could be the result of species in the reaction flask that led to the hydrolysis of the **DHA-Cl**. The presence of water or NaOH that remained from the basification of **^{OH}PyNMe$_3$** in the step prior to the attachment of the fatty acid could lead to the hydrolysis of the fatty acyl chloride. For future attempts of attachment of a fatty acyl chloride to **^{OH}PyNMe$_3$**, it is recommended that the basification of **^{OH}PyNMe$_3$** is accomplished with K_2CO_3 so that if there is residual base in the reaction, it would not lead to the hydrolysis of the acyl chloride. These results indicate a need to modify the last steps in the attachment of the fatty acid to the macrocycle.

Experimental

I. General experimental notes

General Methods. All reagent and solvents were obtained from commercial sources and used as received unless noted otherwise. All reactions were carried out under inert atmosphere. Deionized ultrapure water was obtained from a four-stage Millipore filter system and used to prepare all solutions. ^{1}H NMR spectra were recorded at 400 MHz on a Bruker Avance spectrometer using deuterated solvents, and spectra were referenced using TMS as a reference in $CDCl_3$ (in parts per million e.g., TMS δ = 0.00 ppm) and the corresponding residual solvent resonance (in parts per million; e.g., H_2O, δ = 4.79 ppm). For proper identification of the NMR signals, the following abbreviations were used: s = singlet, d = doublet, t = triplet, q = quartet, and m = multiplet. When noted, purification of the compounds was accomplished with column chromatography using silica gel (porosity 60 Å, particle size 40-63 μm). Thin Layer Chromatography (TLC) plates were developed using iodine or UV light (λ = 254 nm) when possible.

II. PAMPA-BBB assay

PAMPA-BBB experiments of compounds were conducted via a PAMPA Evolution96^{TM} instrument (commercial assay by Pion, Inc.). The permeability of each compound was determined in buffers of varying pH of 4.5, 7.4, and 10.0. In PAMPA, a sandwich is formed such that each composite well is divided into two chambers, separated by a 125 μm microfilter disc (0.45 μm pores), coated with Pion BBB-1 phospholipid mixture. At the start of the test, the drug-free acceptor compartment was filled with acceptor buffer (BSB) containing a chemical scavenger. The proprietary chemical scavenger mimics sink conditions due to

binding compounds to the brain tissue and effectively eliminates ABL in the acceptor compartment. The aqueous solutions of studied compounds were created by diluting and thoroughly mixing 3 μL of DMSO stock in 600 μL of Prisma HT buffer. The reference solution is identical to the donor at time zero, so that any surface adsorption effects from the plastic ware is compensated. The PAMPA sandwich was assembled and allowed to incubate for 20 ± 5 hours. The sandwich was then separated, and both the donor and receiver compartments were assayed for the amount of drug present by comparison with the UV spectrum obtained from reference standards. Mass balance was used to determine the amount of material remaining in the membrane filter and on the plastic (%R). Sample powders of ^{OH}**PyN$_3$** and ^{OH}**Py$_2$N$_2$** pre-weighed in glass vials were brought to the room temperature at the day of the experiment. The samples were diluted with organic solvent DMSO to prepare stock solutions at concentration ~20mM. The stock solution for ^{OH}**PyN$_3$** appeared slightly turbid. Solution was vortexed and sonicated for few minutes to insure a homogeneous particles distribution and was introduced in the experiment. The stock solution for ^{OH}**Py$_2$N$_2$** appeared clear; no precipitation was observed at room temperature. The stock solutions were further diluted with buffers at pH values 4.5, 7.4 and 10.0 producing the aqueous samples` solutions at concentrations ~100 μM. The amount of DMSO in the resulting solution was <0.5% (v/v). After permeation, the sandwich is disassembled and the UV spectra are scanned from 190 nm to 500 nm. The spectrum of a reference solution is used to determine the relative concentration in both the donor and acceptor. The permeability coefficients are then calculated from these relative concentrations.

III. Computational analysis methods

Computational analyses were conducted utilizing a Molinspiration™ software that predicts properties of a molecule based on the structure inputted into the program. LogBB was calculated according to methods previously reported by Dr. Mi Hee Lim and coworkers (logBB = -0.0148 x PSA + 0.152 x *c*log*P* + 0.13).[27] The values obtained for logBB were utilized to predict whether or not the given target molecule would be found in the CNS.

IV. Synthetic procedure for Diethyl 4-(hexanoyloxy)-2,6-pyridinedicarboxylate

Synthesis of diethyl 4-(hexanoyloxy)-2,6-pyridinedicarboxylate (1). Diethyl chelidamate (2.01 g, 8.41 mmol), K_2CO_3 (1.39 g, 10.0 mmol), and CH_2Cl_2 (50 mL) was added to a two-neck 250-mL round-bottomed flask. Hexanoyl chloride (1.13 g, 8.37 mmol) was added dropwise to the reaction mixture and stirred. A condenser was placed on the top of the flask and the reaction mixture was refluxed. After 40 h, the flask was cooled to room temperature and the solvent was removed under reduced pressure. Water (50 mL) was added to the flask and the mixture was extracted with EtOAc (50 mL × 5). The organic extracts were combined, dried over anhydrous Na_2SO_4, and concentrated under reduced pressure to obtain the **1** (2.74 g, 8.00 mmol, 95%) as a tan oil, which solidified after 2 days on standing. NMR ($CDCl_3$, δ/ppm): ^{1}H (400 MHz) 8.03 (s, 2H), 4.45 (q, 4H J = 7.2 Hz), 2.58 (t, 2H, J = 7.6 Hz), 1.73 (quintet, 2H, J = 7.4 Hz), 1.46-1.28 (m, 10H), 0.89 (t, 3H, J = 7.1 Hz); ^{13}C ($CDCl_3$, 101 MHz) 170.5, 164.0, 159.3, 150. 5, 121.1, 62.5, 34.2, 31.1, 24.3, 22.2, 14.2, 13.8.

V. Synthetic procedure for DHA attached SES protected $^{OH}PyN_3$

Synthesis of diethyl 4-hydroxy-2,6-pyridinedicarboxylate (2). Chelidamic acid **(1)** (20.4 g, 0.111 mol) was added to a 500-mL round-bottom flask with 200 mL of abs. EtOH. The flask was then cooled to 0° C. Thionyl chloride ($SOCl_2$) (23.7 mL, 0.327 mol) was added dropwise to the reaction flask with an addition funnel. After complete addition, the reaction mixture was refluxed at 80° C for 4 h. The oil bath was removed and the reaction was continued at rt overnight. The mixture was concentrated using a water aspirator pump and the resulting dark brown oil was rinsed with toluene (2 x 100 mL) and the solvents were removed using rotary evaporation. Na_2CO_3 and water (40 mL) were added to the resulting oil. Diethyl ether (40 mL) was added to the oil to promote crystallization. The resulting crystals were isolated by vacuum filtration. The isolated solid crystals were then dissolved in $CHCl_3$. The resulting mixture was placed on top of a silica gel column and washed with $CHCl_3$. The fractions containing the product were collected and the solvent was evaporated to obtain **2** as a white solid (19.7 g, 82.3 mmol, 74%). NMR ($CDCl_3$, δ/ppm): ^{1}H (400 MHz) 7.16 (s, 2H), 4.49 (q, 4H, J = 8.0 Hz), 1.71 (br s, 1H, OH), 1.45 (t, 6H, J = 4.0 Hz).

Synthesis of diethyl 4-[(tetrahydro-2*H*-pyran-2-yl) oxy]-2,6-pyridinedicarboxylate (3). 2 (5.04 g, 21.1 mmol) and CH_2Cl_2 (70 mL) was added to a 3 neck 250 mL round-bottom flask. 3,4-dihydro-2*H*-pyran (7.87 mL, 86.1 mmol) and p-toluenesulfonate (PPTS) (0.529 g, 2.11 mmol) was added and the mixture was refluxed. After 16 h, the mixture was cooled and washed with brine (2 × 20 mL) followed by water (2 × 20 mL). The organic fractions were dried (Na_2SO_4). The solvent was then evaporated under reduced pressure to yield a tan oil. This oil was dried overnight using oil pump vacuum to obtain a white precipitate. The resulting crude solid was purified by flash column chromatography (R_f = 0.24, SiO_2, CH_2Cl_2:EtOAc =

15:1 with 1% triethylamine). The product containing fractions were collected and the solvent was removed under reduced pressure. Hexane was added to the resulting yellow oil and a white solid formed upon sonication. The mixture was cooled to -35 °C to facilitate precipitation. The precipitate was isolated by vacuum filtration and dried using oil pump vacuum to obtain **3** as a white solid (5.06 g, 15.6 mmol, 74%). NMR ($CDCl_3$, δ/ppm): ^{1}H (400 MHz) 7.94 (s, 2H), 5.71 (t, 1H, J = 2.8 Hz), 4.49 (q, 4H, J = 8.0 Hz), 3.80 (td, 1H, J = 11.2, 2.8 Hz), 3.69 (dtd, 1H, J = 11.6, 4.8, 1.6 Hz), 2.08 – 1.66 (m, 6H), 1.48 (t, 6H, J = 7.2 Hz).

Synthesis of 4-[(tetrahydro-2*H*-pyran-2-yl) oxy]-2,6-pyridinedimethanol (4). 3 (5.05 g, 15.6 mmol) and abs. EtOH (50 mL) was added to a 250-mL round-bottom flask and the mixture was cooled to 0 °C. Sodium borohydride (3.10 g, 81.9 mmol) was added to the reaction mixture in portions. The resulting reaction mixture was stirred at 0 °C for 1 h and 25°C for 2 h. The condenser was placed on the top of flask and the mixture was refluxed overnight. The mixture was cooled and the solvent was evaporated under reduced pressure to obtain a waxy solid. Acetone (60 mL) was added and the mixture was refluxed for 1 h. The mixture was cooled and the solvent was evaporated under reduced pressure. A solution of K_2CO_3 (16 g in 45 mL of water) was added to the residue and the mixture was refluxed for 2 h. The solvent was then concentrated under reduced pressure and brine (15 mL) was added to the residue. The mixture was extracted with chloroform (3 × 45 mL). The organic layers were combined and dried over anhydrous Na_2SO_4 and then concentrated under reduced pressure to give a light yellow solid, which was dried overnight using oil pump vacuum to obtain a sticky white solid. The solid was washed with hexanes and dried to obtain **4** as a white solid (1.70 g, 7.10 mmol, 46%). NMR (MeOD, δ/ppm): ^{1}H (400 MHz) 7.10 (s, 2H), 5.66 (t, 1H, J = 2.8 Hz), 4.63 (s, 4H), 3.83 (td, 1H, J = 10.6, 3.2 Hz), 3.65 (dtd, 1H, J = 11.2, 4.4, 1.2 Hz), 2.10 – 1.42 (m, 6H).

Synthesis of 4-[(tetrahydro-2*H*-pyran-2-yl)oxy]-2,6-pyridinedimethyl ditosylate (5). **4** (1.68 g, 7.04 mmol) was vigorously stirred in a mixture of CH_2Cl_2 and 40% aqueous KOH solution (40 mL of each) at 0 °C. Tosyl chloride (2.96 g, 15.5 mmol) was added to the flask in one portion. The resulting reaction mixture was stirred for 1 h at 0 °C and then at room temperature for 4 h. The mixture was then washed into a separatory funnel with water and CH_2Cl_2 (80 mL of each). The resulting mixture was then extracted. The aqueous phase was then shaken with CH_2Cl_2 (3 × 80 mL). The combined organic phases were dried over anhydrous Na_2SO_4 and the solvent was evaporated under reduced pressure to yield a colorless oil. Anhydrous MeOH was added to the crude product and the mixture was then sonicated for 10 minutes to yield **5** as a white precipitate which was then filtered and dried under vacuum (2.65 g, 4.84 mmol, 69%). NMR ($CDCl_3$, δ/ppm): ^{1}H (400 MHz) 7.82 (d, 4H, J = 8.0 Hz), 7.35 (d, 4H, J = 8.0 Hz), 6.98 (s, 2H), 5.51 (t, 1H, J = 2.8 Hz), 5.00 (s, 4H), 3.75 (td, 1H, J = 11.2, 2.8 Hz), 3.64 (dtd, 1H, J = 10.8, 4.0, 1.6 Hz), 2.46 (s, 6H), 2.06 – 1.63 (m, 6H).

Synthesis of sodium 2-(trimethylsilyl) ethanesulfonate (7). Vinyltrimethylsilane **(6)** (38 mL, 26 g, 260 mmol), methanol (100 mL), and tert-butyl perbenzoate (0.99 mL, 1.0 g, 5.2 mmol) was added to a three-neck 500-mL round-bottom flask. To this, a solution of $NaHSO_3$ (52.0 g, 500 mmol) in water (100 mL) was added. The flask was equipped with a reflux condenser, and the resulting suspension was heated in an oil bath at 50 °C under nitrogen for 48 h. The suspension was concentrated under reduced pressure using rotary evaporation followed by azeotropic removal of the residual water with methanol (2 × 35 mL). Methanol (300 mL) was added to the resulting white solid, and the resulting suspension was stirred vigorously for 10 min. The mixture was filtered through a pad of Celite into a 500-mL, round-bottomed flask, and the filtrate was

concentrated on a rotary evaporator. The filter cake was resuspended in 300 mL of methanol and stirred vigorously for 10 min, filtered into the vessel containing the original filtrate, and further concentrated. The preceding operations were repeated again on the filter cake. After the final concentration of the combined filtrates, the resulting white solid was dried to yield **7** containing salts (47.8 g, 0.234 mmol, 90% yield). NMR (DMSO-d_6, δ/ppm): ^{1}H (400 MHz) 3.34 (broad s, OH), 2.32 (AA'XX', 2H, $J_{AA'}$ = 14.2 Hz, $J_{AX'}$ = 13.8 Hz, $J_{XX'}$ = 13.5 Hz, J_{AX} = 4.0 Hz), 0.81 (AA'XX', 2H, $J_{AA'}$ = 14.2 Hz, $J_{AX'}$ = 13.8 Hz, $J_{XX'}$ = 13.6 Hz, J_{AX} = 4.0 Hz), -0.03 (s, 9H). ^{13}C{^{1}H} (101 MHz) 46.5, 11.9, -1.8.

Synthesis of 2-(trimethylsilyl) ethanesulfonyl chloride (8). Sulfuryl chloride (4.6 mL) was added dropwise via an addition funnel to a solution of triphenylphosphine (PPh_3) (13.5 g) in CH_2Cl_2 (20 mL) at 0° C. After the solution was stirred for 10 minutes, a sample of **7** (5.6 g, 27.4 mmol) was added in portions. After the reaction was run for an additional 30 minutes at 0° C, the ice bath was removed and the resulting yellow solution was stirred for 24 hr. The resulting mixture was then added dropwise via an addition funnel to a 500-mL round-bottom flask containing 100 mL of pentanes with vigorous stirring. After 20 minutes of stirring, the suspension was diluted with an additional 100 mL of pentanes. The resulting solution was filtered through a 5.5 cm pad of silica packed with pentanes. The filter cake was washed with a solution of 5% diethyl ether in pentane (1 L). The filtrate was then concentrated under reduced pressure to yield the crude product which was a yellow oil. The oil was then put in the freezer (-20° C) to yield solid crystals of **8** (4.68 g, 23.3 mmol, 85% yield). NMR ($CDCl_3$, δ/ppm): ^{1}H (400 MHz) 3.61 (broad s, OH), 1.31 (AA'XX', 2H, $J_{AX'}$ = 14.3 Hz, $J_{AA'}$ = $J_{XX'}$ = 13.8 Hz, J_{AX}

= 3.9 Hz), 0.81 (AA'XX', 2H, $J_{AX'}$ = 14.3 Hz, $J_{AA'}$ = $J_{XX'}$ = 13.8 Hz, J_{AX} = 3.9 Hz), 0.12 (s, 9H). $^{13}C\{^{1}H\}$ (101 MHz) 63.5, 12.0, -1.9.

Synthesis of 1,4,7-tris[2-(trimethylsilyl) ethanesulfonyl]-1,4,7-triazaheptane (9). A 500-mL round bottom flask was charged with triethylamine (5.22 mL, 0.052 mmol), diethylenetriamine (0.69 mL, 0.006 mmol), and CH_2Cl_2 (20 mL). The mixture was stirred at –20 °C (1:3 NaCl/ice). A solution of **8** (5.72 g, 0.029 mmol) in CH_2Cl_2 (15 mL) at –20 °C was added dropwise to this reaction mixture over ca. 10 min, and the reaction temperature was maintained at –20 °C. After 3 h, the reaction mixture was poured into water (30 mL). The resulting solution was extracted with CH_2Cl_2 (3 × 30 mL). The organic phases were combined, washed with brine (30 mL), and dried using anhydrous Na_2SO_4. The solvent was evaporated using rotary evaporation and the residue was purified using silica gel column chromatography (CH_2Cl_2:EtOAc = 9:1). The product containing fractions was combined and the sample was concentrated to obtain a viscous yellow oil. Hexanes (20 mL) were added, and the mixture was kept at −35 °C for 1 h during which a white precipitate formed. The mixture was filtered to obtain **9** as a white solid (1.029 g, 0.002 mol, 27%). NMR ($CDCl_3$, δ/ppm): ^{1}H (400 MHz) 5.10 (t, 2H), 3.45 (m, 4H), 3.38 (m, 4H), 3.10-2.90 (m, 6H), 1.04 (m, 6H), 0.08 (m, 28H).

Synthesis of SES, THP-protected $^{OH}PyN_3$ (9). 8 (1.427 g, 2.39 mmol) and Cs_2CO_3 (2.34 g, 7.17 mmol) were combined in 30 mL of DMF. A solution of **5** (1.309 g, 2.39 mmol) in 30 mL of DMF was added dropwise. The reaction mixture was stirred at room temperature for 24 h. The solvent was removed under reduced pressure using rotary evaporation, and the residue was transferred to a separatory funnel with CH_2Cl_2 (70 mL) and water (70 mL). The aqueous solution was extracted with CH_2Cl_2 (2 × 70 mL). The combined organic extracts were washed with brine (70 mL), dried over anhydrous

Na_2SO_4, filtered, and concentrated under reduced pressure. The resulting yellow oil was purified by column chromatography (SiO_2, CH_2Cl_2:EtOAc = 20:1 with 1% TEA, R_f = 0.8) to yield **9** as a white solid (63% yield). NMR ($CDCl_3$, δ/ppm): ^{1}H (400 MHz) 7.10 (s, 2H), 5.57 (t, 1H, J = 2.8 Hz), 4.44 (m, 4H), 3.77 (td, 1H, J = 11.0, 2.8 Hz), 3.68-3.60 (m, 1H), 3.60-3.45 (m, 4H), 3.12 (broad s, 4H), 2.97 (AA'XX', 4H, $J_{AX'}$ = 14.2 Hz, J_{AX} = 3.8 Hz, $J_{AA'}$ = $J_{XX'}$), 2.82 (AA'XX', 2H, $J_{AX'}$ = 14.1 Hz, J_{AX} = 3.9 Hz, $J_{AA'}$ = $J_{XX'}$), 2.03-1.83 (m, 3H), 1.03 (AA'XX', 4H, $J_{AX'}$ = 14.2 Hz, J_{AX} = 3.8 Hz, $J_{AA'}$ = $J_{XX'}$), 0.92 (AA'XX', 2H, $J_{AX'}$ = 14.1 Hz, J_{AX} = 3.9 Hz, $J_{AA'}$ = $J_{XX'}$), 0.07 (s, 18H), 0.01 (s, 9H). ^{13}C{^{1}H} (101 MHz) 165.5, 157.1, 111.7, 96.1, 62.2, 55.4, 49.4, 48.5, 47.4, 47.2, 29.7, 24.8, 18.2, 10.3, 10.2, -1.96.

Synthesis of SES-protected ^{OH}PyN$_3$ (10). 9 (1.00 g, 1.25 mmol) was dissolved in a mixture of CH_2Cl_2 (50 mL) and MeOH (50 mL). PPTS (0.31 g, 1.25 mmol) was added in one portion and the resulting solution was refluxed under nitrogen for 18 h. The solvents were evaporated under reduced pressure and the resulting colorless oil was washed into a separatory funnel with CH_2Cl_2 (60 mL). The organic phase was washed with 150 mL of H_2O:brine mixture (1:1). The aqueous phase was then extracted with CH_2Cl_2 (2 × 60 mL). The organic fractions were combined and dried with anhydrous Na_2SO_4. The solvent was then evaporated under reduced pressure using rotary evaporation. The resulting off-white foamy solid was purified by column chromatography (SiO_2, CH_2Cl_2:EtOAc = 2:1, $R_f \sim 0.7$) yielding colorless oil which solidified under vacuum overnight, to form **10** as white crystalline solid (94% yield). NMR ($CDCl_3$, δ/ppm): ^{1}H (400 MHz) 7.19 (s, 2H), 4.72 (s, 4H), 3.74 (m, 4H), 3.51 (m, 4H), 3.10 (AA'XX', 4H, $J_{AA'}$ = $J_{XX'}$ = 14.3 Hz, $J_{AX'}$ = 14.2 Hz, J_{AX} = 3.8 Hz), 2.87 (AA'XX', 2H, $J_{AX'}$ = 13.9 Hz, J_{AX} = 3.8 Hz, $J_{AA'}$ = $J_{XX'}$), 1.05 (AA'XX', 4H, $J_{AX'}$ = 14.2 Hz, J_{AX} = 3.8 Hz,

$J_{AA'} = J_{XX'}$), 0.93 (AA'XX', 2H, $J_{AX'}$ = 14.1 Hz, J_{AX} = 3.9 Hz, $J_{AA'} = J_{XX'}$), 0.07 (s, 18H), 0.04 (s, 9H). $^{13}C\{^{1}H\}$ (101 MHz) 173.2, 150.8, 111.1, 56.0, 52.6, 45.9, 41.4, 9.6, 8.8, -2.1, -2.2.

Synthesis of docosahexaenoyl chloride (11). A 50-mL Schlenk flask was charged with $SOCl_2$ (0.2 mL, 2.64 mmol), CH_2Cl_2 (5 mL), and stirred. The flask was cooled to 0 °C and *cis*-4,7,10,13,16,19-Docosahexaenoic acid (**DHA**) (0.318 g, 0.001 mmol) was added dropwise. The mixture was stirred for 2 h at 0 °C. The excess thionyl chloride was removed under vacuum at room temperature to obtain **11** as a tan oil. It was upon analyzing the resulting NMR, it was determined that **11** was not fully synthesized and instead the oil reflected starting material. This indicated that this synthetic pathway could not be used to synthesize **DHA-Cl**.

Synthesis of DHA appended, SES-protected $^{OH}PyN_3$ (12). A solution of **10** (0.436 g, 0.600 mmol) in CH_2Cl_2 (15 mL) was added to a 100-mL round-bottom and stirred at 0 °C. Triethylamine (0.45 mL, 0.003 mol) was added to the flask followed by dropwise addition of **11** (0.23 g, 0.700 mmol) in CH_2Cl_2 (5 mL). The ice bath was removed, and the mixture was stirred for 16 h at room temperature. The solvents were removed and the crude mixture. CH_2Cl_2 was added and the mixture was washed with $NaHCO_3$ (2 × 25 mL), brine (25 mL), and H_2O (2 × 25 mL). It was at this step that it was determined by a co-worker in the laboratory that the SES group could not be removed from the macrocycle successfully. Thus, this synthetic step was not characterized and this pathway was abandoned as a synthetic route towards achieving a fatty acid appended macrocycle.

VI. Synthetic procedure for fatty acid-appended ^{OH}PyNMe$_3$

Synthesis of diethyl 4-hydroxy-2,6-pyridinedicarboxylate to 4-[(tetrahydro-2*H*-pyran-2-yl) oxy]-2,6-pyridinedimethyl ditosylate (2 – 5). The synthetic methods for intermediates **2** – **5** are the same as was previously reported in the synthetic procedure for **DHA** appended, SES-protected ^{OH}**PyN$_3$**.

Synthesis of 1,4,7-Tris(2-nitrobenzenesulfonyl)-1,4,7-triazaheptane (7). A three-necked round-bottom flask was charged with 2-nitrobenzenesulfonyl chloride (25.10 g, 0.113 mol) in CH_2Cl_2 (300 mL) and stirred. Diethylenetriamine **(6)** (3.8 mL, 0.035 mol) and triethylamine (8.3 mL, 0.060 mmol) in CH_2Cl_2 (100 mL) were added dropwise to this mixture. The mixture was stirred at room temperature for 20 h. The solvent was concentrated using rotary evaporation to obtain an orange mixture, which was washed with sat, aqueous $NaHCO_3$. The organic layer was extracted with H_2O (3 × 75 mL), dried over anhydrous Na_2SO_4, and the solvent was removed under reduced pressure to yield an orange foam. The crude product was recrystallized from CH_2Cl_2/$CHCl_3$ (9:1) to give **7** as an off-white solid (21.87 g, 0.033 mmol, 95%). NMR (DMSO-d_6, δ/ppm): ^{1}H (400 MHz) 3.04 (t, 4H), 3.36 (t, 4H), 7.77 (m, 12 H). ^{13}C{^{1}H} (101 MHz): 42.0, 48.6, 125.2, 125.3, 130.1, 130.3, 131.7, 133.0, 133.3, 133.4, 134.8, 135.4, 148.2.

Synthesis of THP, Ns-protected ^{OH}PyN$_3$ (8). 5 (2.30 g, 4.12 mmol) was added to a 250-mL round-bottom flask with anhydrous DMF (60 mL). This resulting solution was added dropwise to a mixture of **7** (2.90 g, 4.39 mmol) and Cs_2CO_3 (5.77 g, 17.7 mmol) in anhydrous DMF (60 mL) in a 3-neck 250 mL round-bottom flask. The mixture was stirred at room temperature overnight. Toluene (5 × 200 mL) was added and the solvents were removed using rotary evaporation. CH_2Cl_2 (125 mL) was added and the mixture was washed 0.1 M NaOH (1

× 125 mL) and with water (2 × 125 mL). The organic phase was then separated and was washed again with 15% brine (1 × 125 mL). The organic layer was separated and dried over anhydrous Na_2SO_4. The organic layer was concentrated using rotary evaporation to yield a yellow oil. Ethyl acetate (3 × 100 mL) was added to the oil and was removed using rotary evaporation to yield a yellow solid. The resulting solid was then vacuum filtered and rinsed with 0.1 M NaOH (30 mL), water (30 mL), and diethyl ether (30 mL). The resulting solid was placed dried under vacuum overnight to obtain **8** as a yellow solid (3.09 g, 3.59 mmol, 87%). NMR ($CDCl_3$, δ/ppm): ^{1}H (400 MHz) 8.09 – 8.02 (m, 3H), 7.75 – 7.60 (m, 9H), 7.11 (s, 2H), 5.55 (t, 1H, J = 2.8), 4.54 (s, 4H), 3.79 (td, 1H, J = 11.2, 2.8 Hz), 3.67 (dtd, 1H, J = 11.6, 4.44, 0.8 Hz), 3.56 – 3.22 (br m, 8H), 2.04 – 1.63 (m, 6H).

Synthesis of ^{OH}PyN$_3$·3HCl (9). 8 (3.09 g, 3.59 mmol) and K_2CO_3 (5.12 g, 30.7 mmol) in DMF (50 mL) was added to a two-neck, 250-mL round-bottom flask. Thiophenol (1.52 mL, 1.64 g, 14.8 mmol) was added dropwise to this flask with a syringe. The mixture was stirred at room temperature overnight. Toluene (5 × 100 mL) was added to the mixture and the solvent was evaporated under reduced pressure resulting in a dark red oil. The oil was acidified with 1 M HCl (200 mL). This resulting aqueous solution was extracted with CH_2Cl_2 (3 × 100 mL). The aqueous phase was isolated and basified to a pH of 12 with cc. NaOH solution (4 mL). This solvent was removed from the basic aqueous phase via rotary evaporation to obtain a solid residue. Anhydrous MeOH (50 mL) was added to the solid residue and the mixture was vacuum filtered. The filter cake was washed with anhydrous MeOH (3 × 20 mL). The solvent was removed from the combined filtrate to yield a viscous oil. Anhydrous MeOH (10 mL), cc. HCl (4 mL), and diethyl ether (100 mL) were added to the oil and a white

precipitate formed. The resulting mixture was vacuum filtered and the solid was dried overnight using oil pump vacuum to yield **9** as a light-yellow powder containing inorganic salts (2.52 g). NMR (DMSO-d_6, δ/ppm): ^{1}H (400 MHz) 6.92 (s, 2H), 4.47 (s, 4H), 3.40 (s, 4H), 3.29 (s, 4H).

Synthesis of ^{OH}PyNMe$_3$ (10). 9 (0.595 g, 1.79 mmol) was added to a 10-mL round-bottom flask. To this, a mixture of 37% formaldehyde (2.08 mL, 27.9 mmol), and formic acid (1.28 mL, 27.9 mmol) was added dropwise while the mixture was stirred at 0ºC. The mixture was stirred for 30 minutes at 0ºC, 1 h at RT, 3 h at 80ºC, and 2.5 h at 95ºC. To this reaction mixture, cc NaOH (10 mL) was added resulting in a solution with a pH of 14. The solvent was evaporated via rotary evaporation, yielding a brown solid containing inorganic salts. Cold isopropanol (40 mL) was added to the solid and the flask was sonicated for 15 min. The mixture was then cooled in the freezer for 10 min. The solution was filtered via vacuum filtration. The inorganic salts on the filter were washed with cold isopropanol (3 × 5 mL). The solvent of the resulting filtrate was evaporated using rotary evaporation to yield a yellow solid with impurities. The solution was then extracted with CH_2Cl_2 and 0.1M NaOH (3 × 30 mL). The solvent of the organic phase was then evaporated with rotary evaporation to yield a light-yellow oil. It was initially thought that not all of the product was recovered, so the oil was recombined with the aqueous phase and the aqueous phase was evaporated under reduced to yield a mixture. Acetone (30 mL) was added to the mixture and the resulting mixture was filtered via vacuum filtration. The presence of aqueous NaOH in the solution with acetone led the conversion acetone into diacetone alcohol so this procedural step cannot be used in the future. The solvent of the resulting filtrate was removed via rotary

evaporation. The resulting mixture was then extracted with CH_2Cl_2 and 0.1 M HCl. This step was shown to be unnecessary as it was determined that the initial yellow oil following the first extraction was the clean product. The aqueous phase was evaporated to yield **10** as a yellow oil (0.330 g, 0.883 mmol, 49.3%). NMR (DMSO-d_6, δ/ppm): ^{1}H (400 MHz) 6.79 (s, 2H), 4.46 (s, 4H), 3.30 (m, 4H), 3.01 (s, 6H), 2.30 (m, 4H), 2.25 (m, 4H).

Synthesis of Docosahexaenoyl chloride (11). The synthesis of docosahexaenoyl chloride was based on a modified procedure proposed by Kamenecka *et al*.[34] Docosahexaenoic acid (0.284 mL, 0.268 g, 0.817 mmol) and CH_2Cl_2 (15 mL) was added to a 50-mL round-bottom flask and stirred at 0ºC. To this mixture, oxalyl chloride (0.080 mL, 0.124 g, 0.979 mmol) was added. One drop of catalytic DMF was added while the reaction was stirred at 0ºC. The ice bath was removed and the reaction was stirred for 2 h at RT. The solvent was then removed under reduced pressure via rotary evaporation to yield **11** as a crude residue which was then utilized immediately for the next step in the synthetic pathway. Because this intermediate could not be characterized due to the reactivity of the **DHA-Cl**, it was undetermined if this reaction was successful.

Synthesis of DHA appended ^{OH}PyNMe$_3$ (12). 10 (0.180 g, 0.680 mmol) and K_2CO_3 (0.565 g, 4.09 mmol) was added to a 50-mL round-bottom flask and dissolved in acetonitrile (20 mL) and stirred at RT. To this mixture, a solution of **11** in acetonitrile (10 mL) was added and stirred at RT for 16 h. The solvent was then removed under reduced pressure via rotary evaporation. The resulting oil was then extracted with CH_2Cl_2 and H_2O (5 × 50 mL). The organic phase was then extracted once more with CH_2Cl_2 and saturated NaCl (5 × 50 mL). The organic phase was then dried over anhydrous $NaSO_4$. The solvent was then removed under

reduced pressure via rotary evaporation to yield a dark brown oil. Upon analysis of the NMR, it was observed that the organic phase contained only **DHA** and not the attached macrocycle. These results indicated the need to append **DHA** to ^{OH}**PyNMe$_3$** through a different synthetic procedure.

Conclusions

As a result of the efforts of this project, a new ligand, **^{OH}PyNMe$_3$**, was synthesized and subsequently characterized utilizing novel synthetic procedures that improved yields and purities of intermediates. The ability of this ligand to form ester and ether linkages opens the possibility of further modification of **^{OH}PyNMe$_3$** with various natural molecules that can increase the BBB permeability of these molecules. In this specific project, an ester linkage was attempted to be synthesized on the pyridoxal moiety of **^{OH}PyNMe$_3$** with the omega-3 fatty acid, **DHA**. The results of a computational analysis of this fatty acid appended ligand show promising predictions that this molecule could have the potential to be found in the CNS where this potential pharmaceutical would be active in combatting neurodegenerative diseases such as AD. The synthetic hurdles to accomplishing this ester appendage have proved to be difficult to overcome. Attempts to esterify the pyridoxal function of **^{OH}PyNMe$_3$** have been unsuccessful to date. The results of a model reaction indicate that a pyridoxal moiety can be esterified. Future work on this synthetic pathway should focus on different methods of successfully converting the omega-3 fatty acid to the corresponding fatty acid chloride. If this can be successfully synthesized and characterized, it should be possible to successfully esterify the pyridoxal moiety of **^{OH}PyNMe$_3$**. The subsequent esterification should be achieved if the only possible reactive center towards the acyl chloride is the pyridoxal function. Care should be made to ensure anhydrous conditions to prevent hydrolysis of the acyl chloride. A different solvent other than acetonitrile, such as DMF, could be utilized for this final attachment. Once this target molecule is successfully synthesized, further studies will need to be conducted *in vitro* to assess the permeability of **DHA** appended **^{OH}PyNMe$_3$**. The results of this work indicate a

need for further investigation into the attachment of various biologically relevant molecules to ^{OH}**PyNMe$_3$**.

Supplementary Appendix

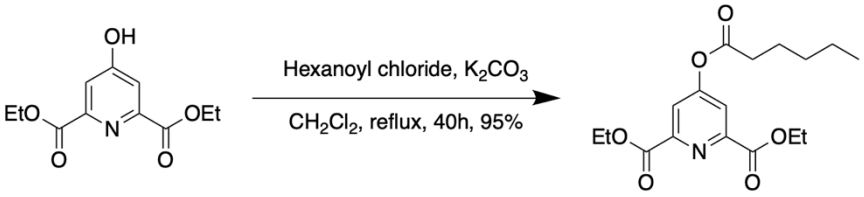

Scheme S1: Synthetic pathway of diethyl 4-(hexanoyloxy)-2,6-pyridinedicarboxylate.

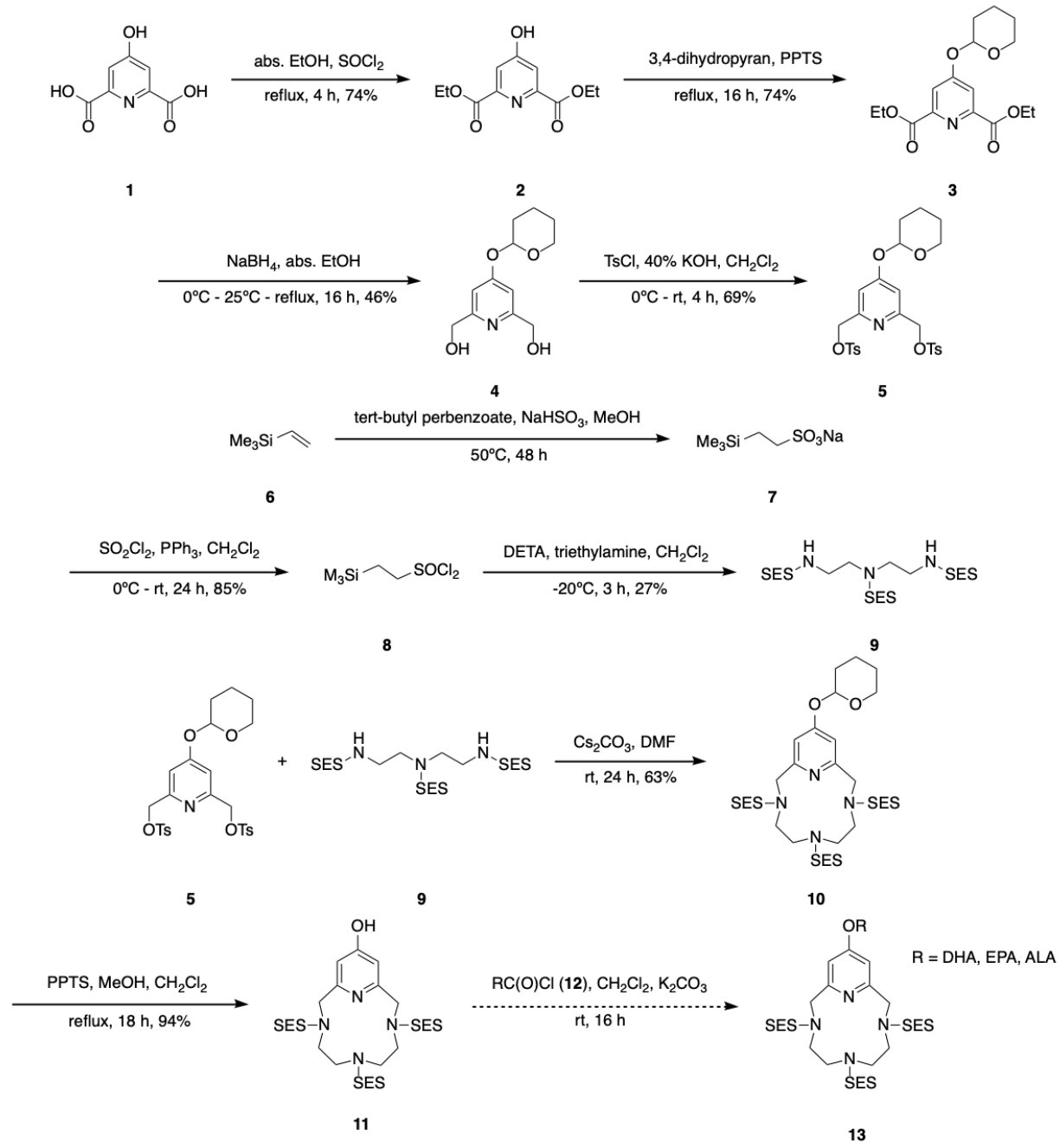

Scheme S2: Synthetic pathway of SES protected, fatty acid attached $^{OH}PyN_3$.

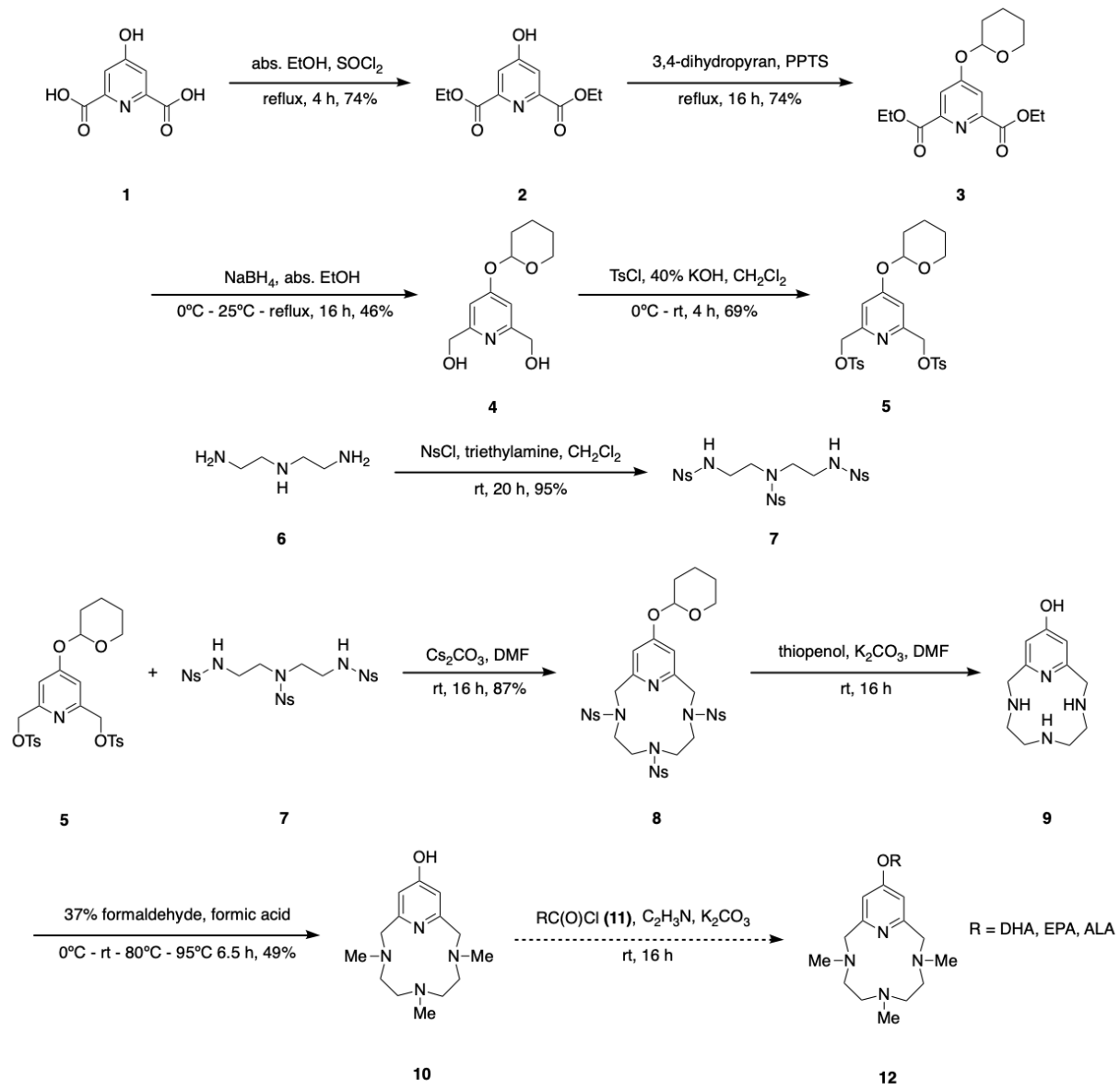

Scheme S3: Synthetic pathway of fatty acid appended ^{OH}**PyNMe3**.

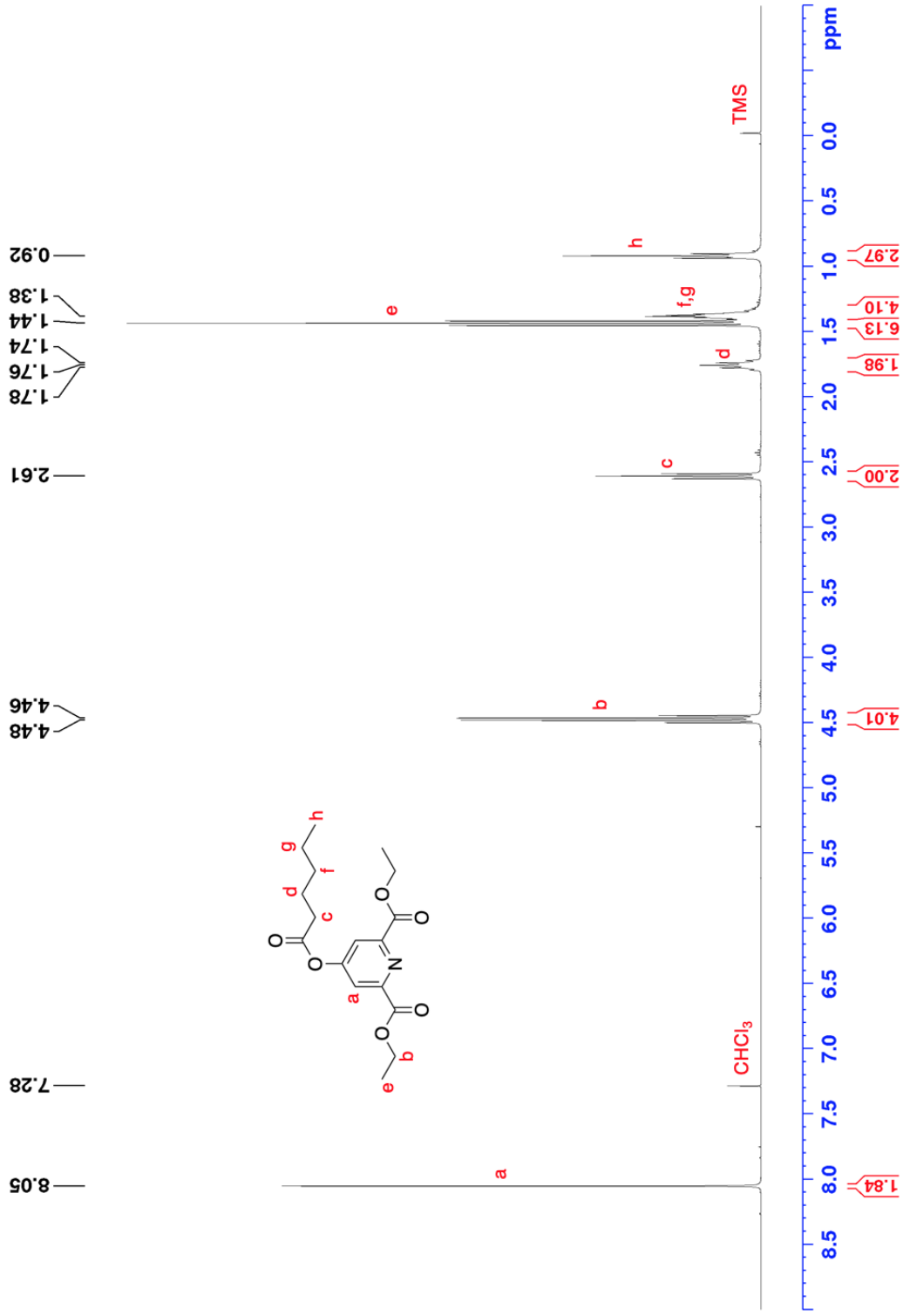

Figure S1: ^{1}H NMR of diethyl 4-(hexanoyloxy)-2,6-pyridinedicarboxylate in $CDCl_3$ at 25°C.

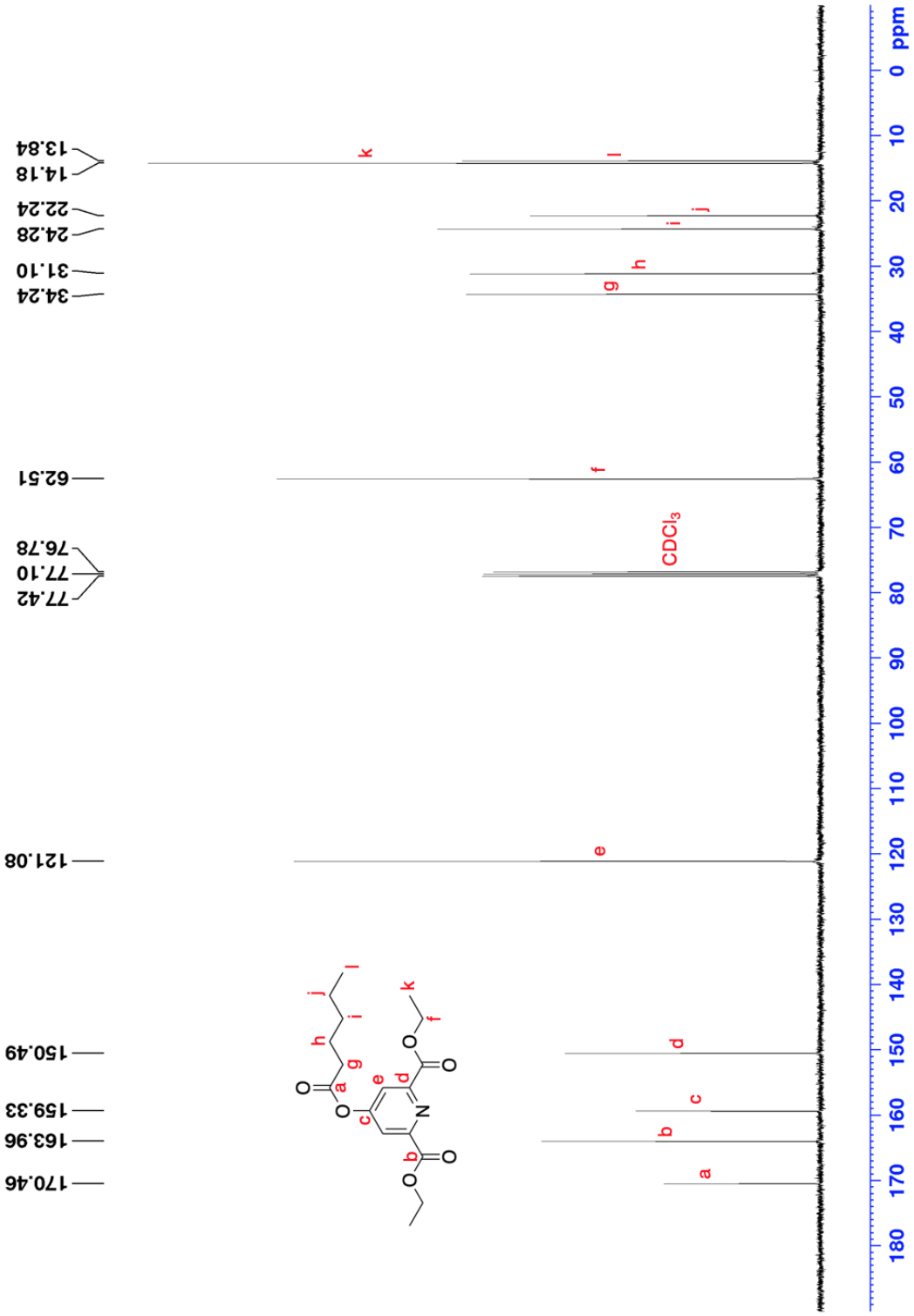

Figure S2: ^{13}C NMR of diethyl 4-(hexanoyloxy)-2,6-pyridinedicarboxylate in $CDCl_3$ at 25°C.

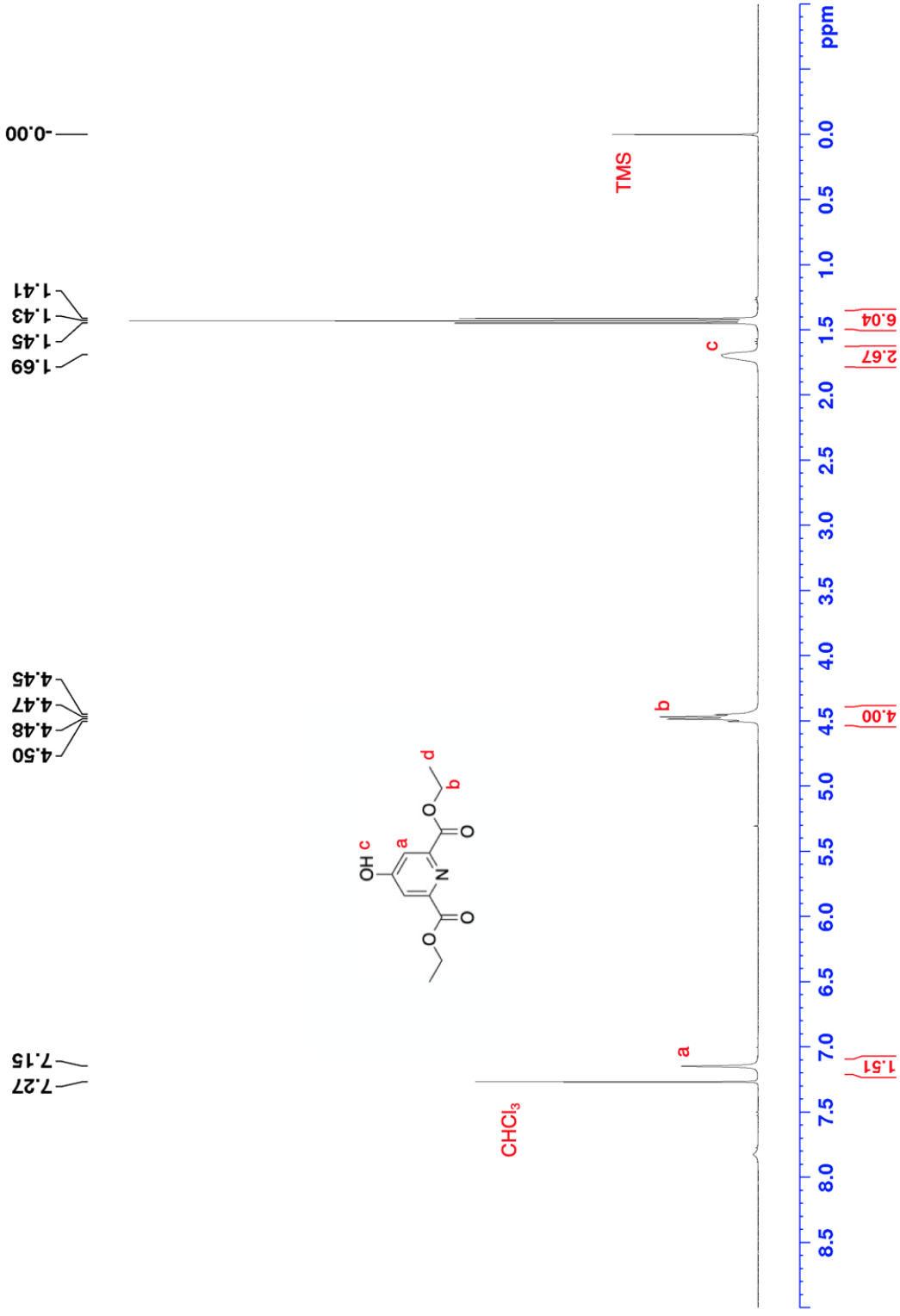

Figure S3: ^{1}H NMR of diethyl 4-hydroxy-2,6-pyridinedicarboxylate **(2)** in $CDCl_3$ at 25°C.

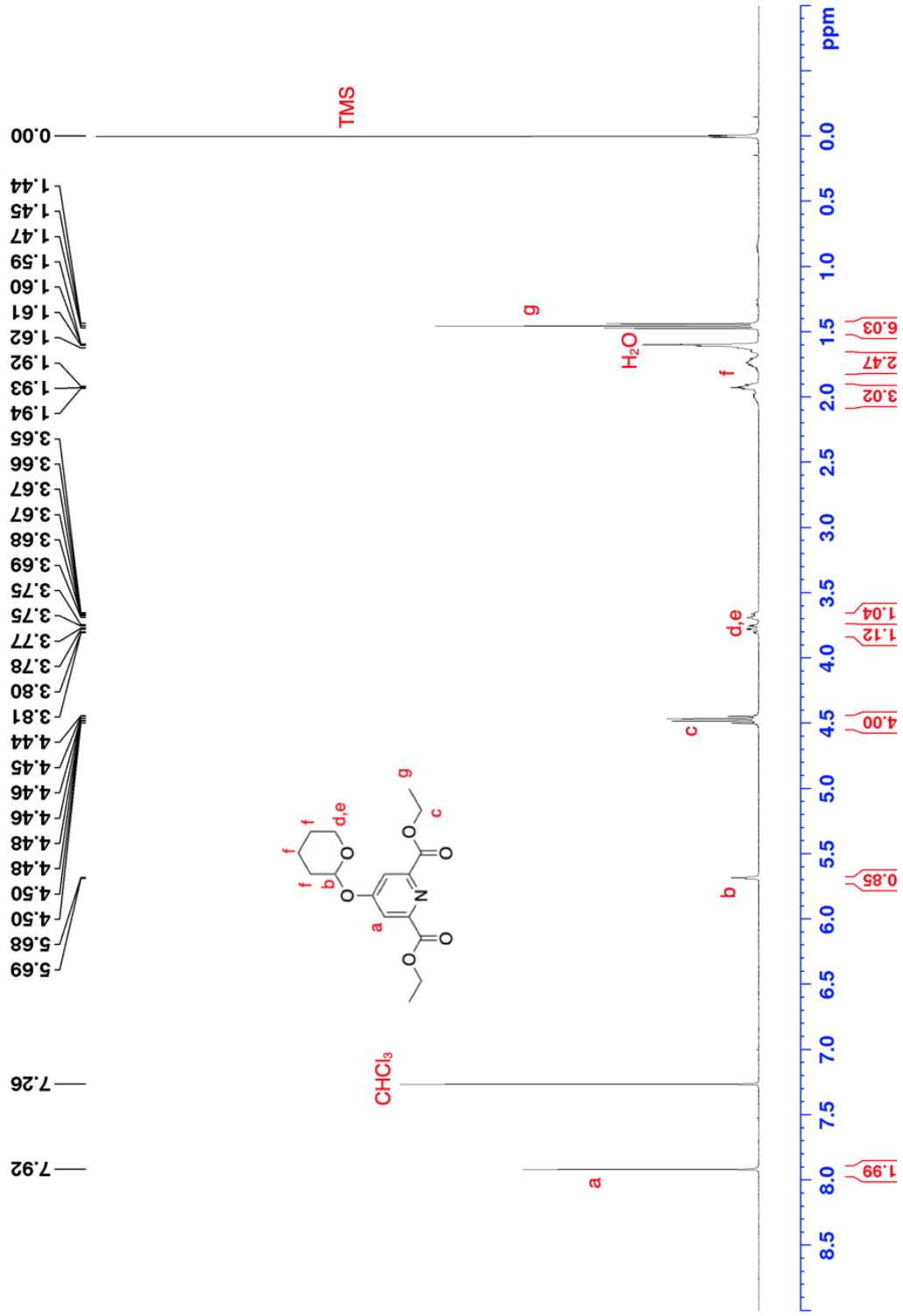

Figure S4: ^{1}H NMR of diethyl 4-[(tetrahydro-2*H*-pyran-2-yl) oxy]-2,6-pyridinedicarboxylate **(3)** in $CDCl_3$ at 25°C.

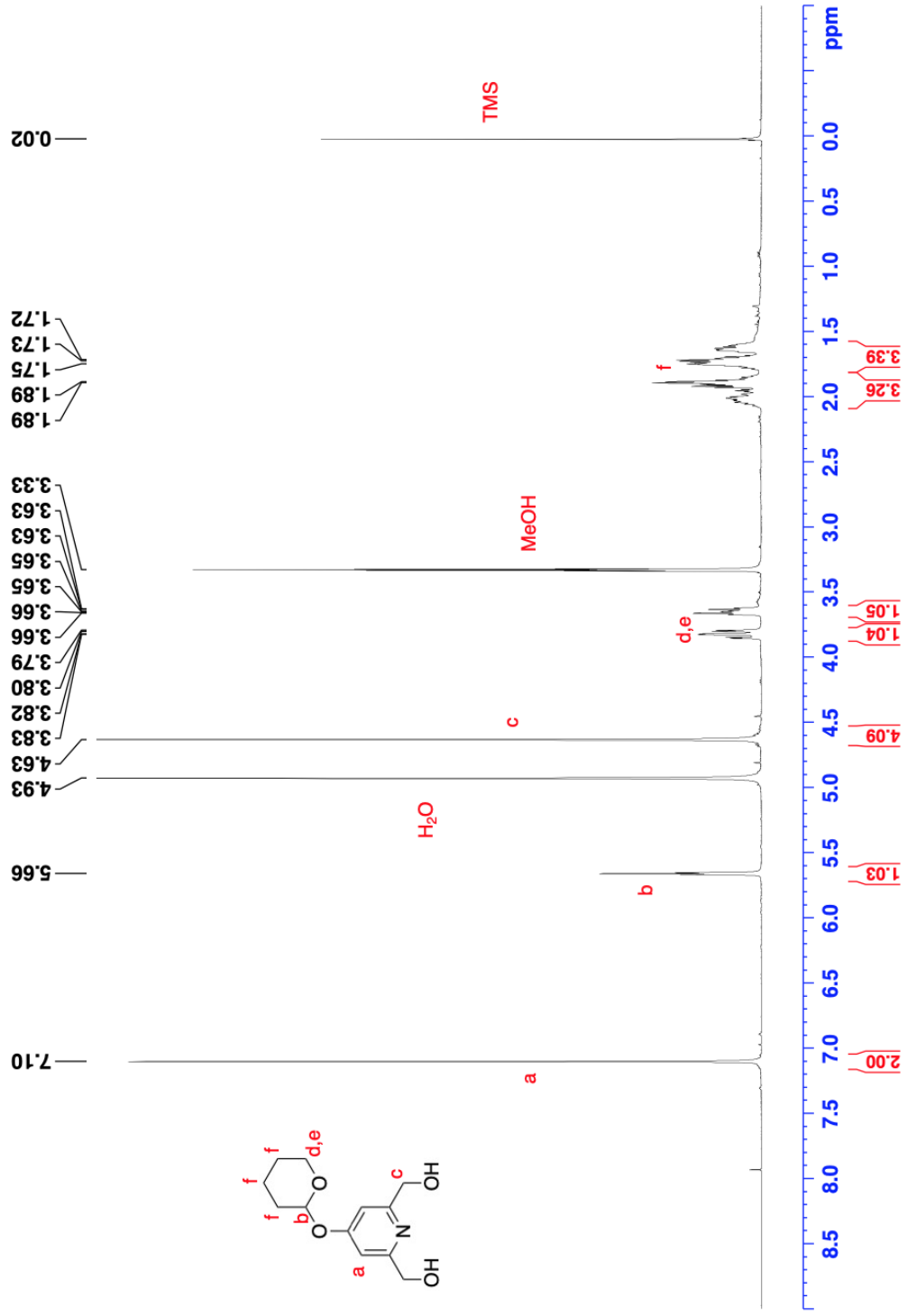

Figure S5: ^{1}H NMR of 4-[(tetrahydro-2*H*-pyran-2-yl) oxy]-2,6-pyridinedimethanol **(4)** in MeOD at 25°C.

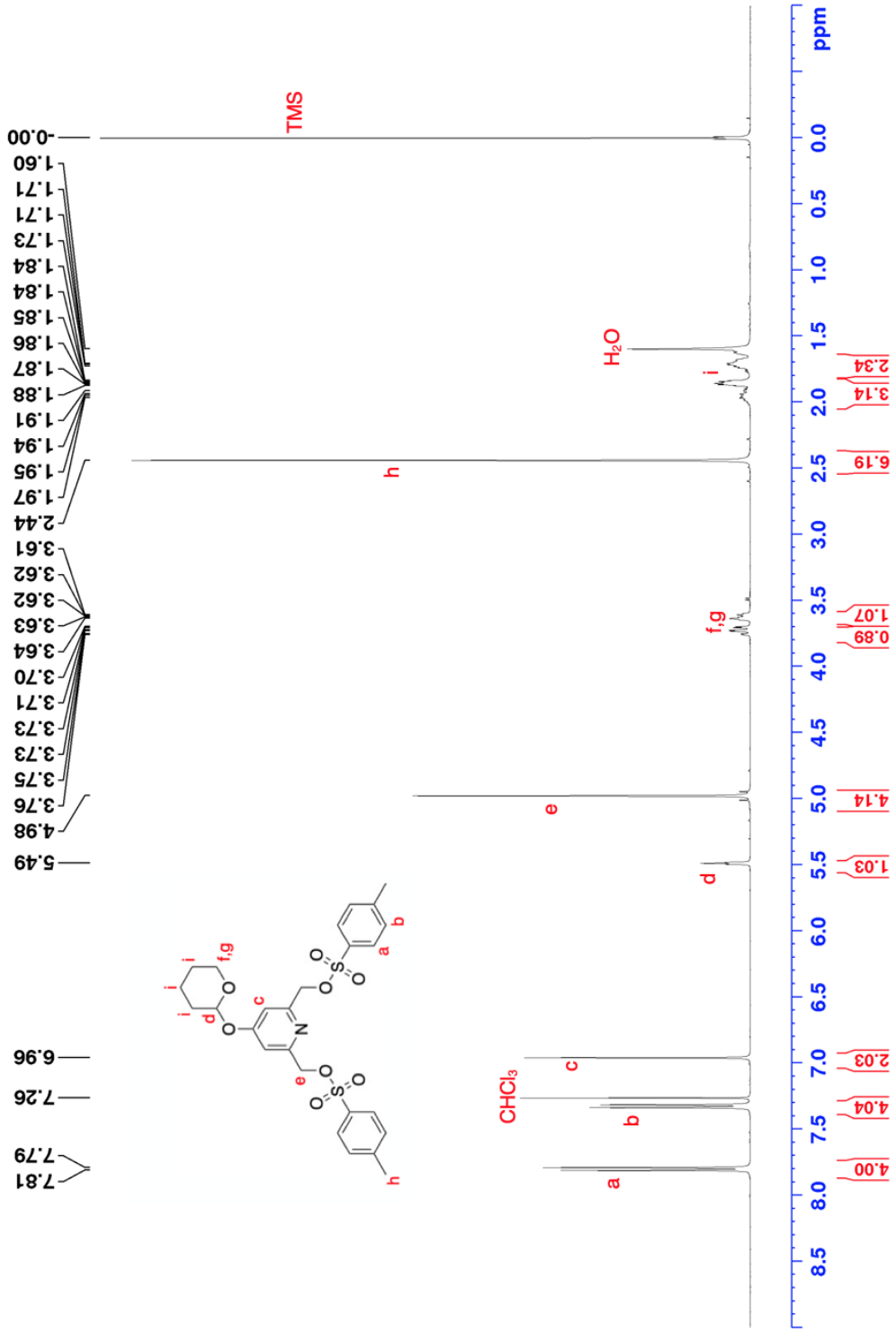

Figure S6: ^{1}H NMR of 4-[(tetrahydro-2*H*-pyran-2-yl) oxy]-2,6-pyridinedimethyl ditosylate **(5)** in $CDCl_3$ at 25°C.

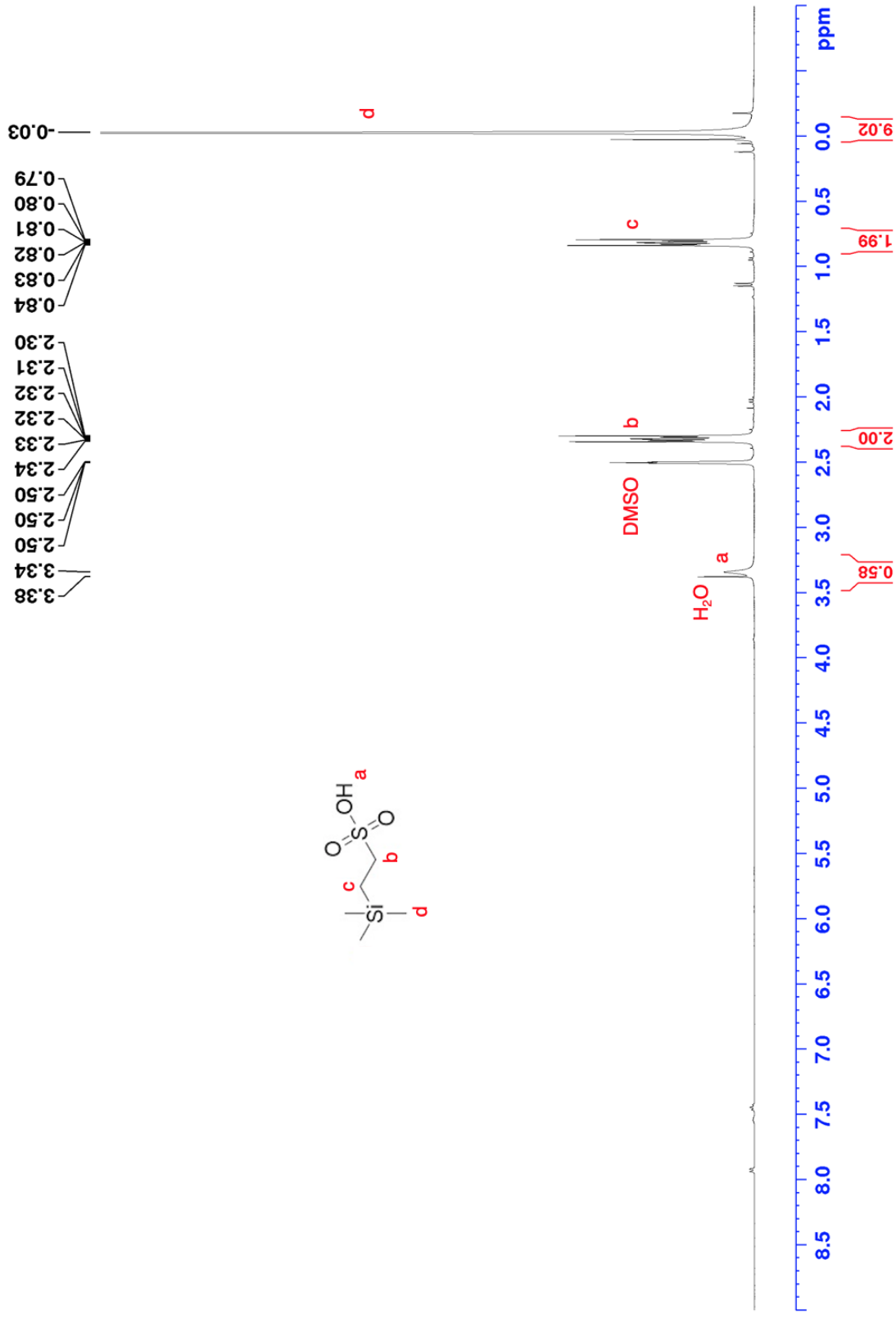

Figure S7: ^{1}H NMR of sodium 2-(trimethylsilyl) ethanesulfonate **(7)** in DMSO at 25°C.

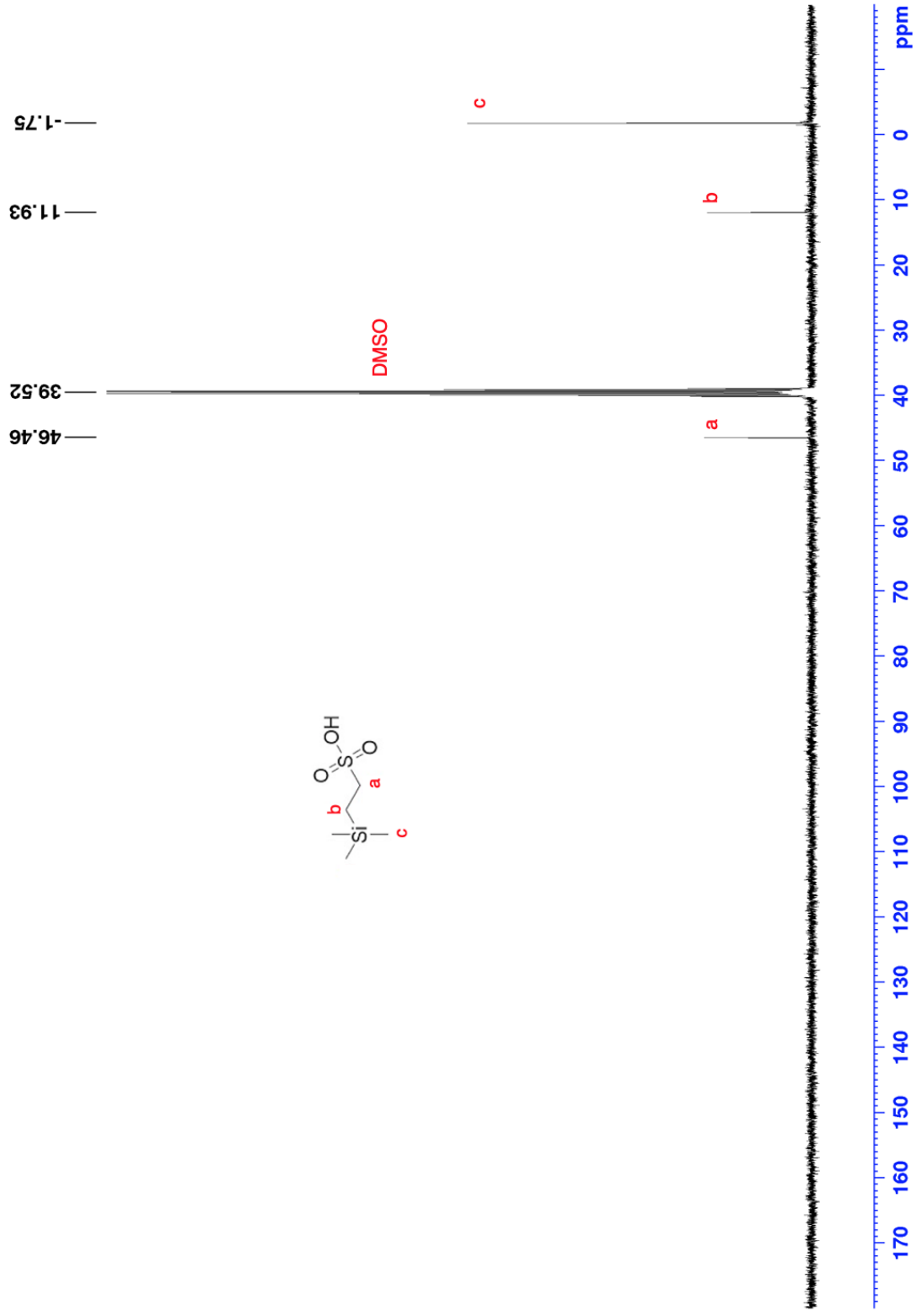

Figure S8: ^{13}C NMR of sodium 2-(trimethylsilyl) ethanesulfonate **(7)** in DMSO at 25°C.

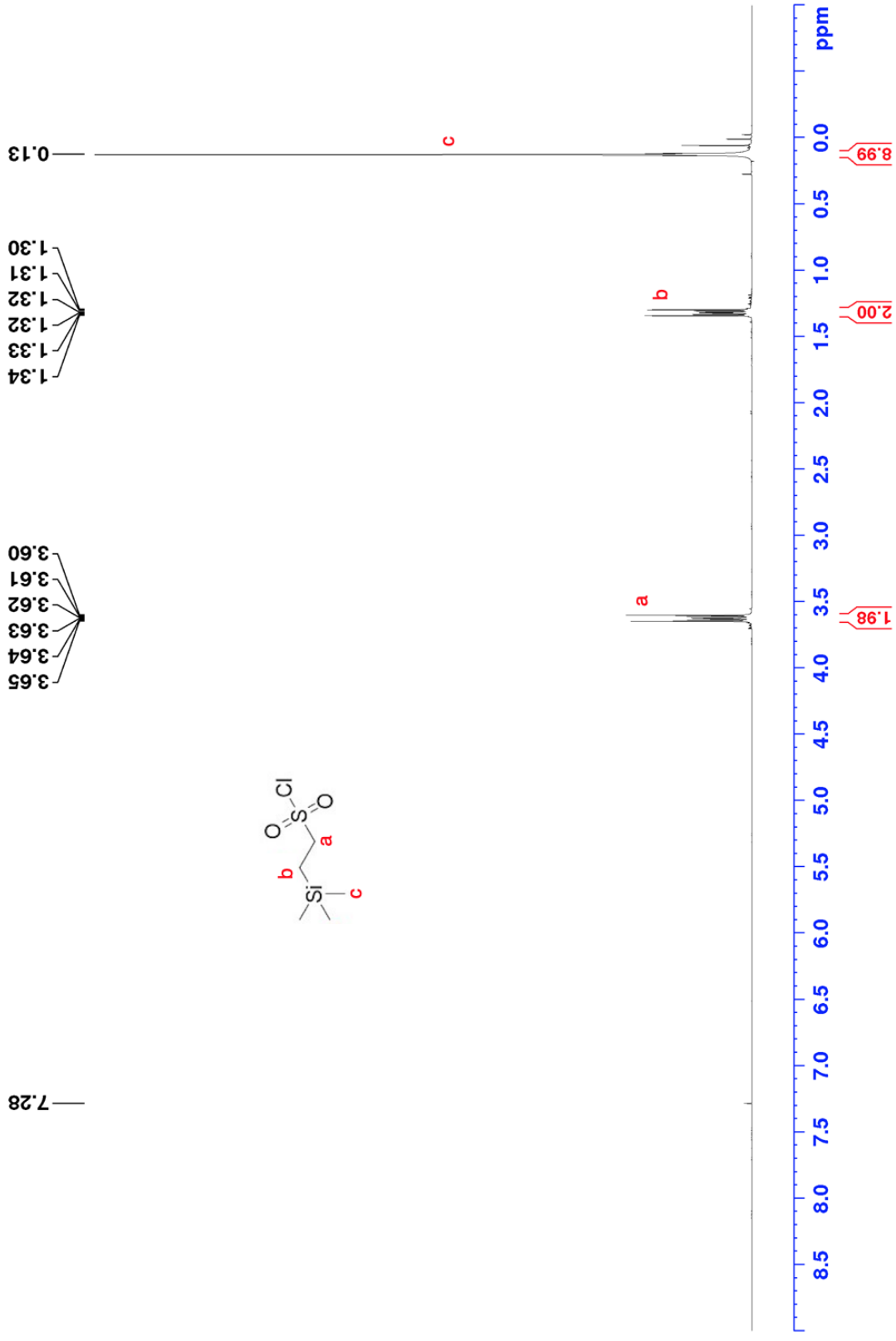

Figure S9: ^{1}H NMR of 2-(trimethylsilyl) ethanesulfonyl chloride **(8)** in $CDCl_3$ at 25°C.

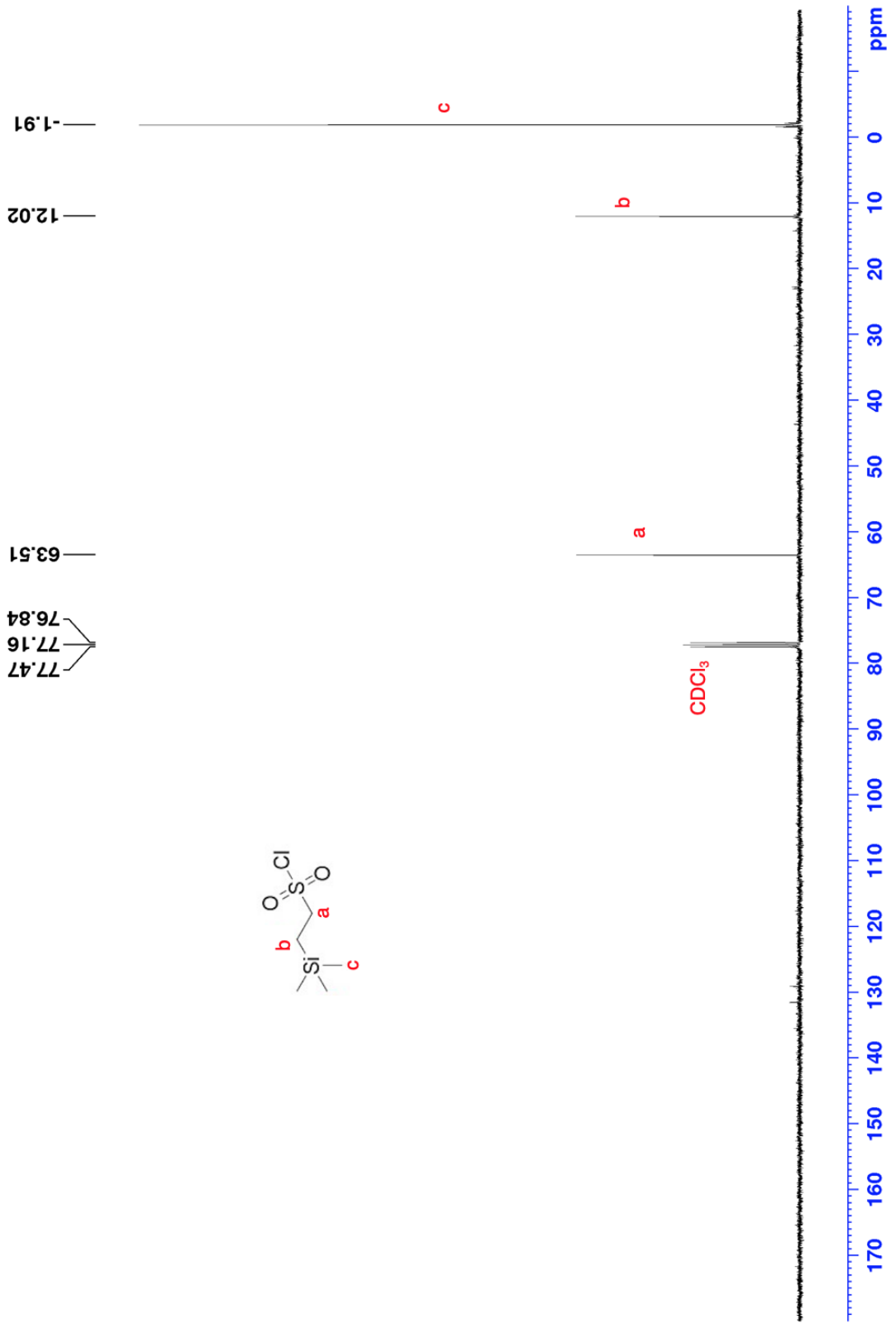

Figure S10: ^{13}C NMR of 2-(trimethylsilyl) ethanesulfonyl chloride **(8)** in $CDCl_3$ at 25°C.

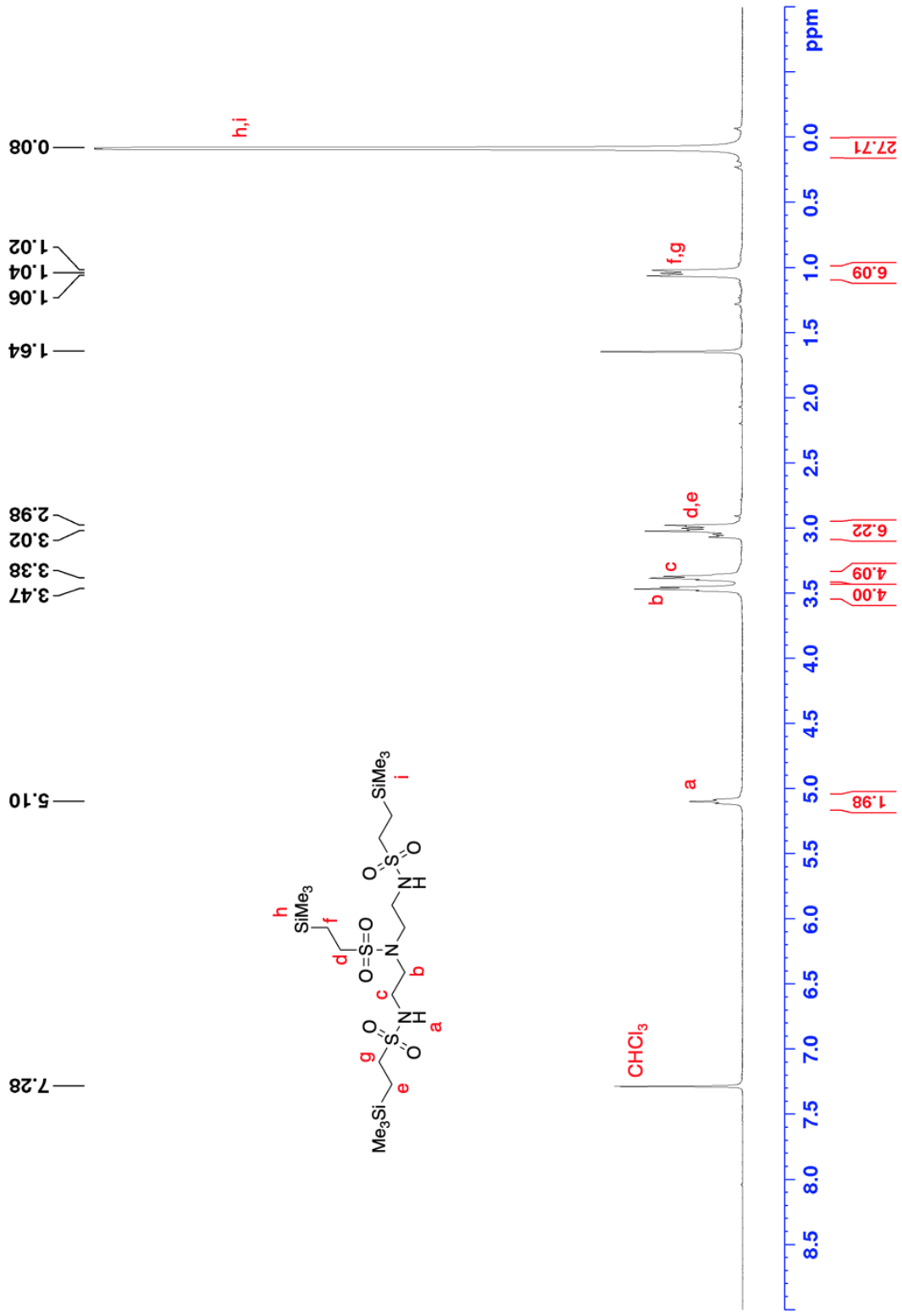

Figure S11: ^{1}H NMR of Synthesis of 1,4,7-tris[2-(trimethylsilyl) ethanesulfonyl]-1,4,7-triazaheptane **(9)** in $CDCl_3$ at 25°C.

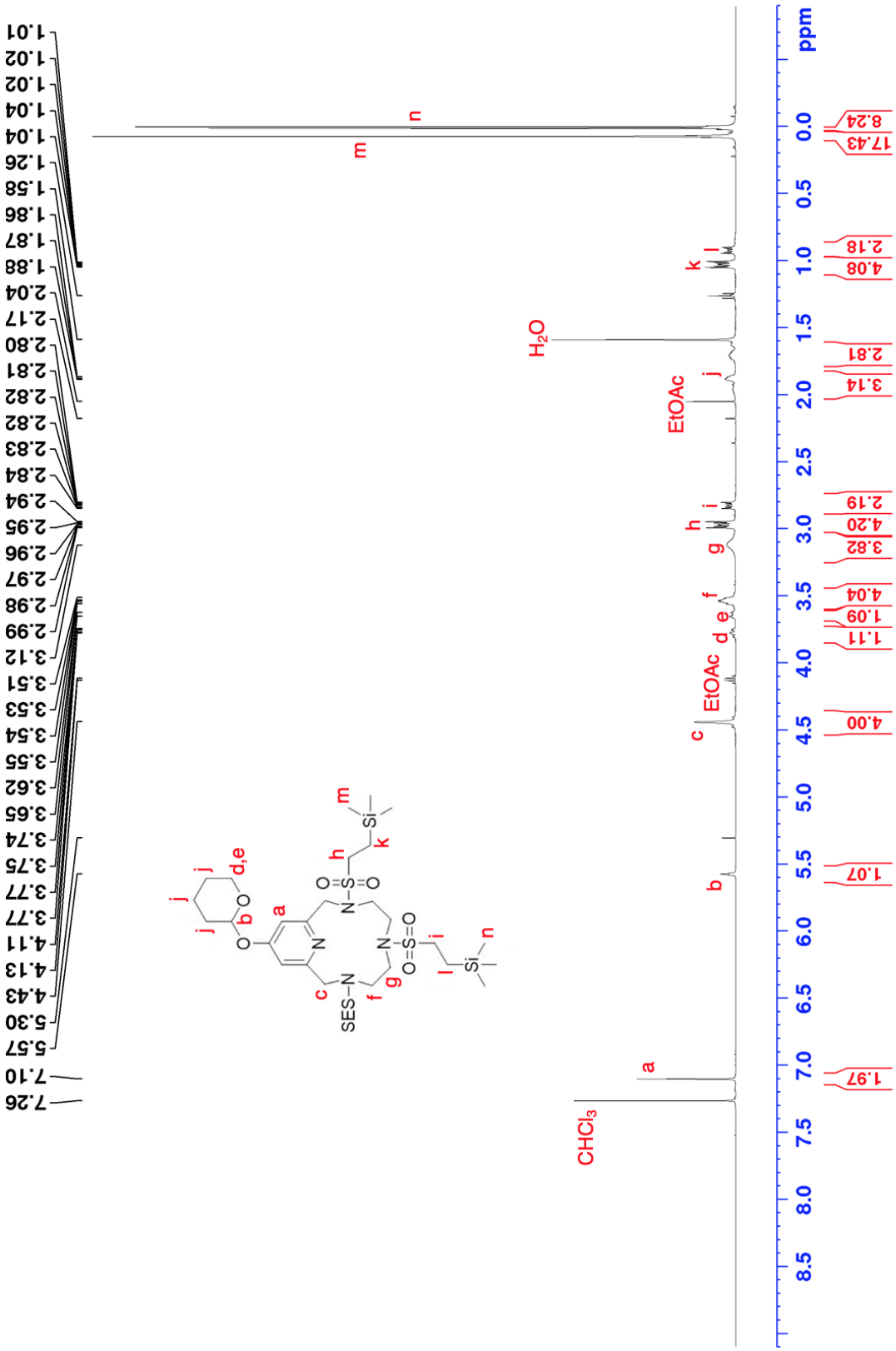

Figure S12: ^{1}H NMR of THP, SES Protected ^{OH}**PyN$_3$ (10)** in $CDCl_3$ at 25°C.

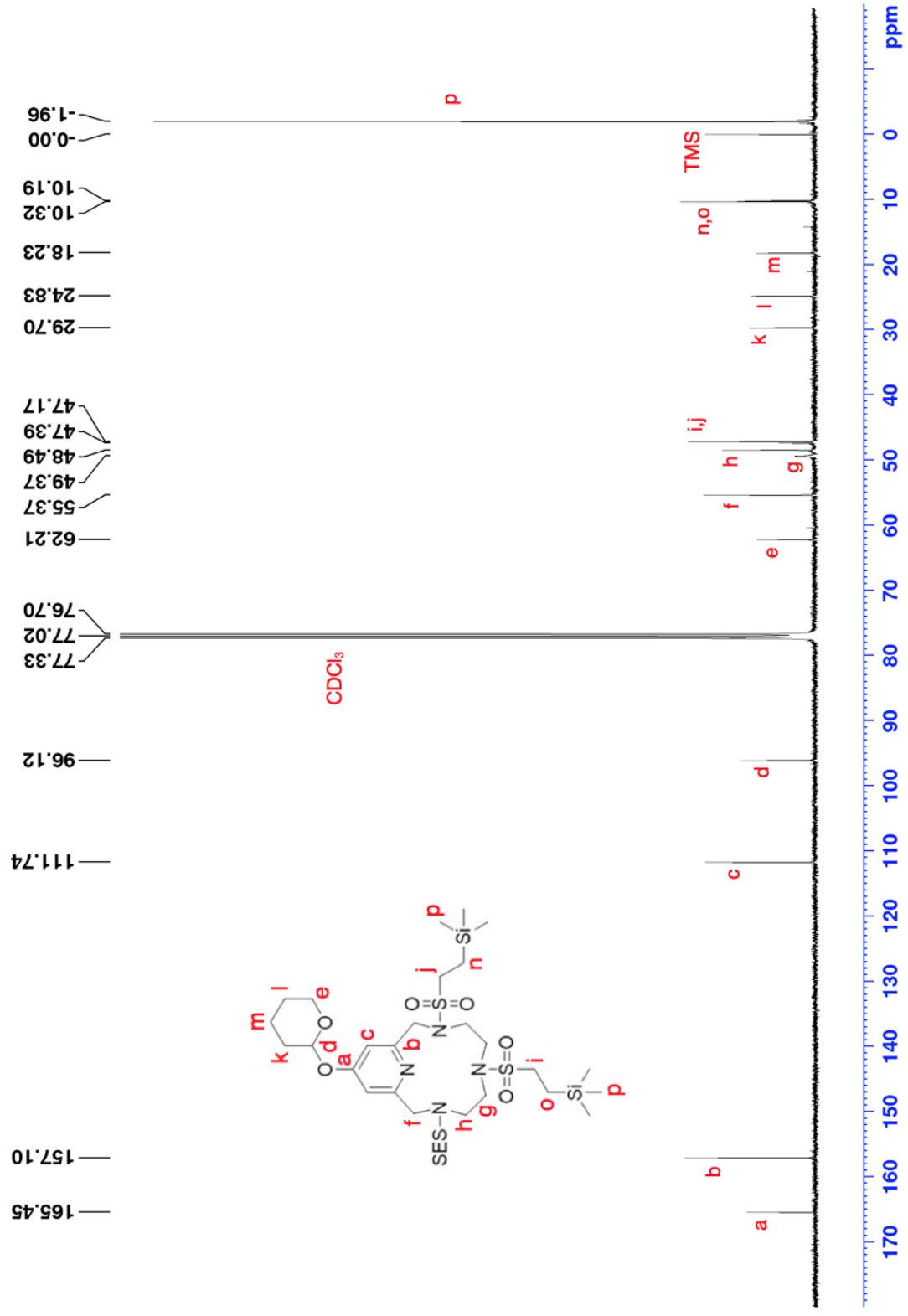

Figure S13: ^{13}C NMR of THP, SES Protected ^{OH}**PyN$_3$ (10)** in $CDCl_3$ at 25°C.

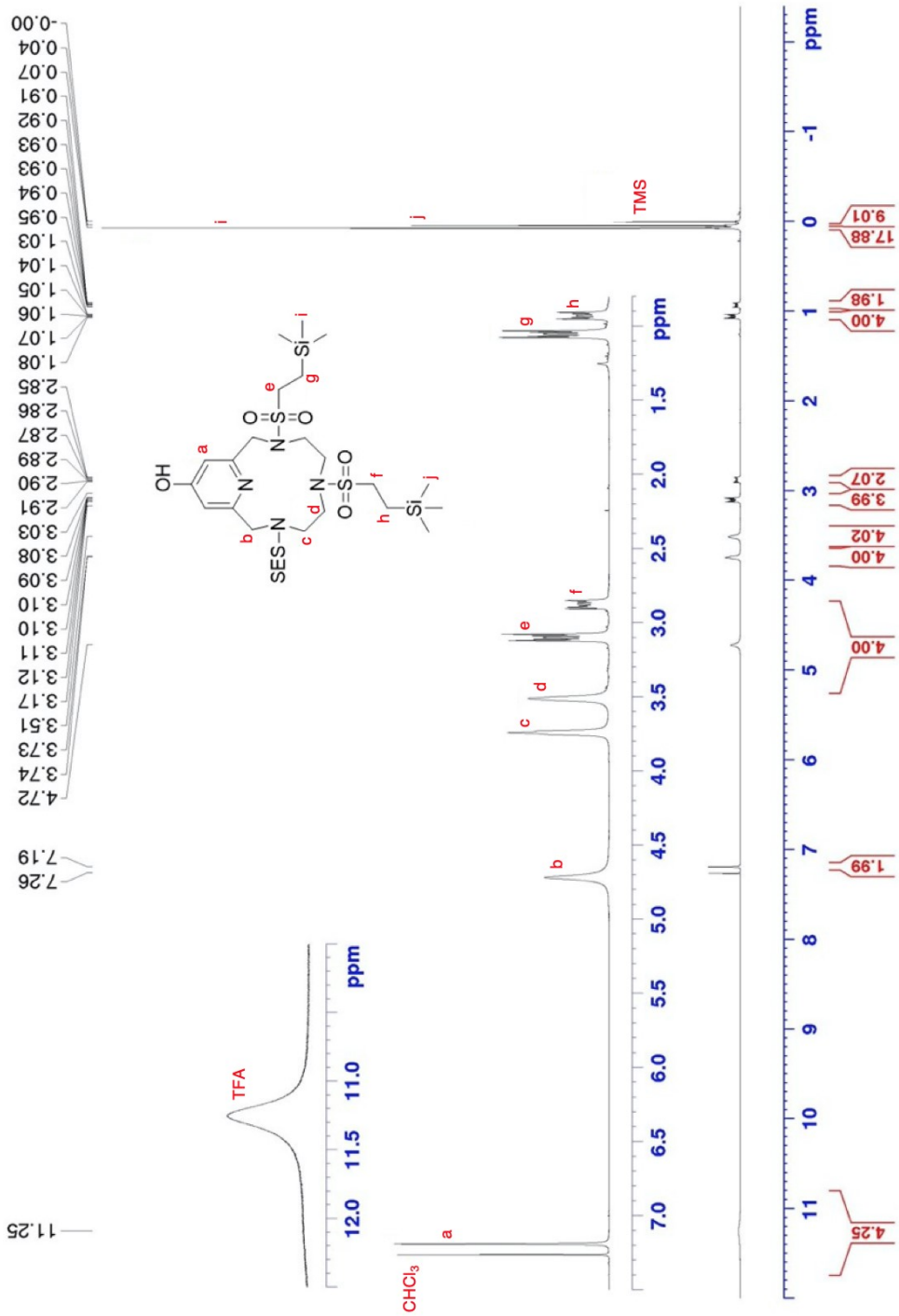

Figure S14: ^{1}H NMR of SES Protected ^{OH}**PyN$_3$ (11)** in $CDCl_3$ at 25°C.

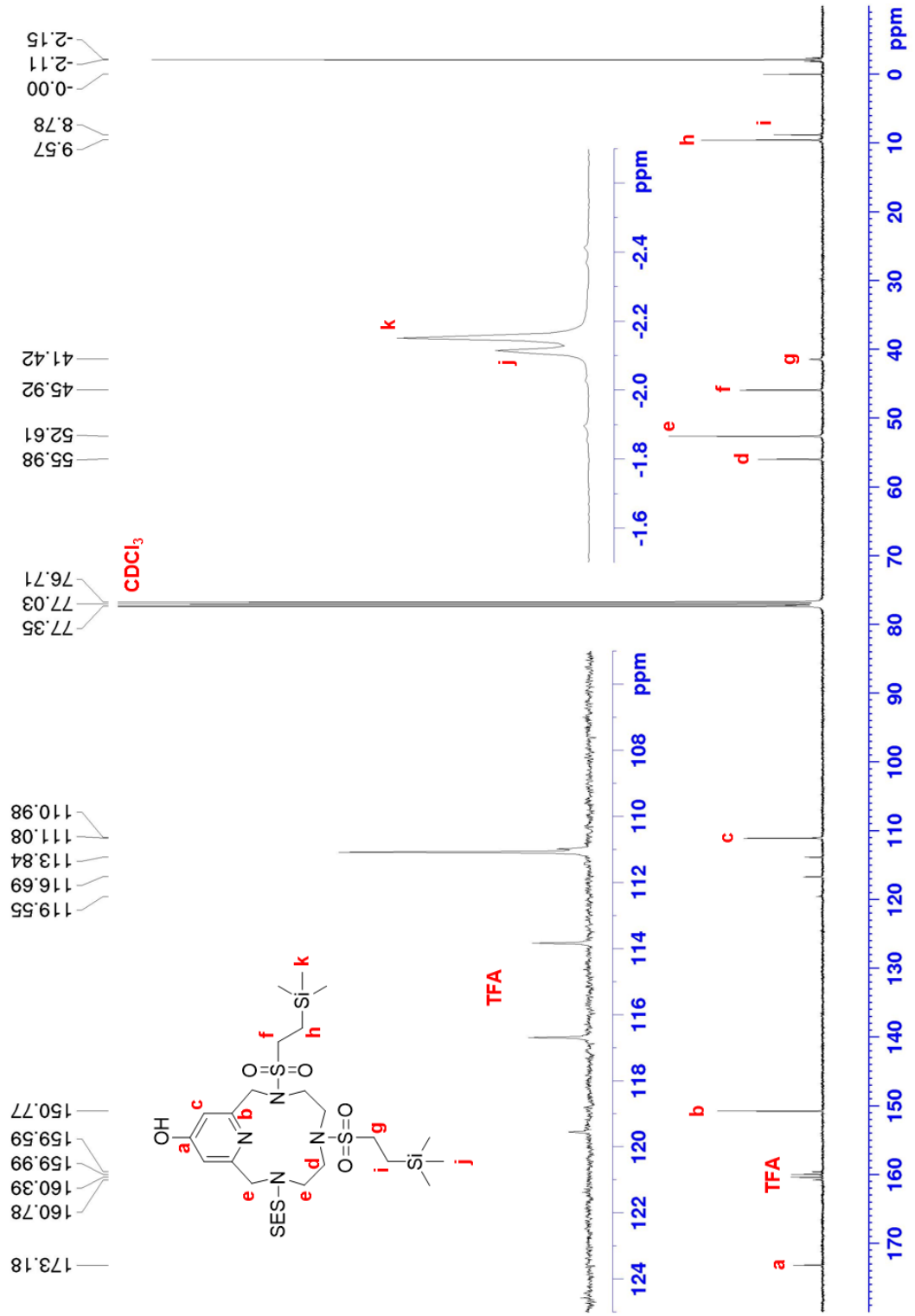

Figure S15: ^{13}C NMR of SES Protected ^{OH}**PyN$_3$ (11)** in $CDCl_3$ at 25°C.

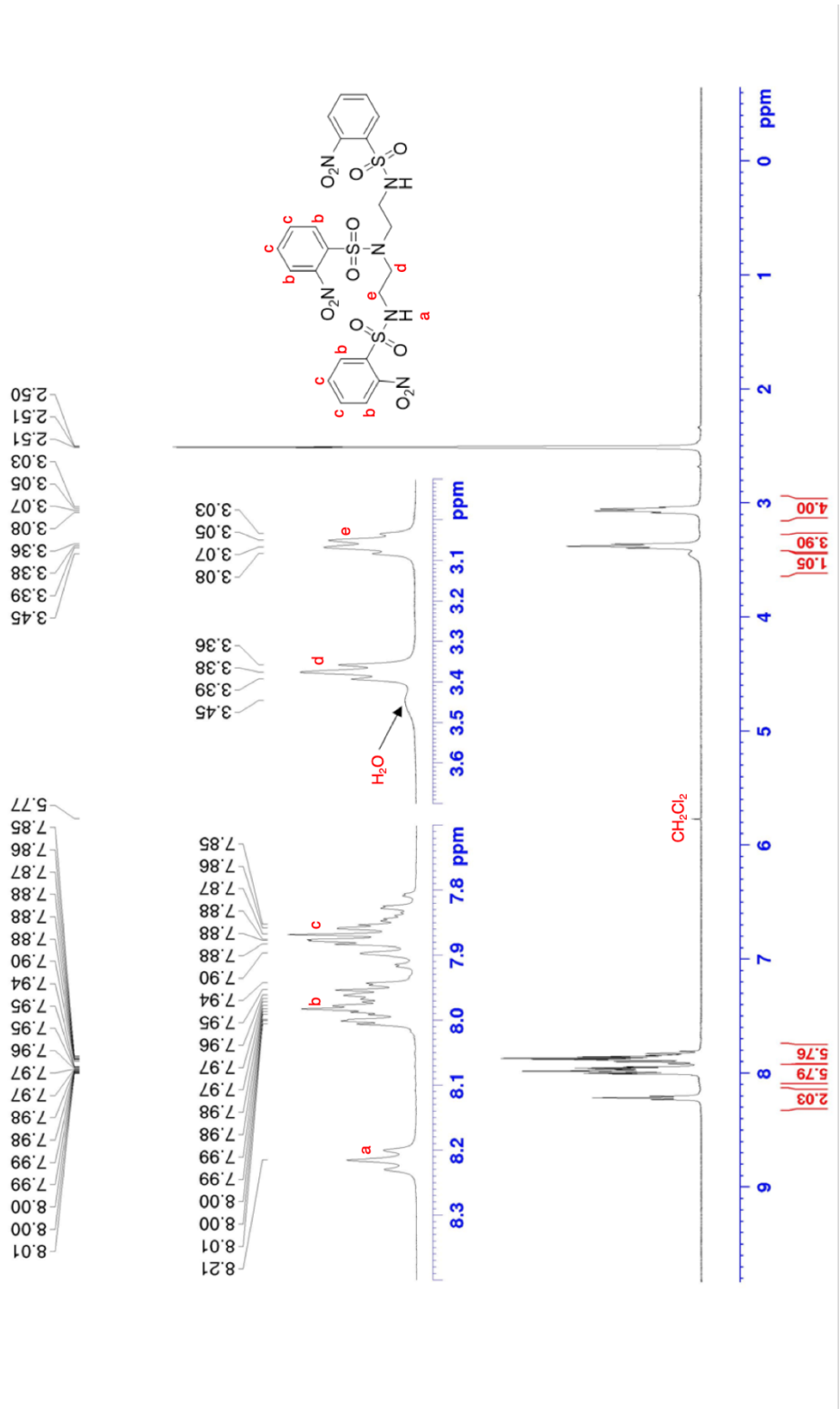

Figure S16: ^{1}H NMR of 1,4,7-Tris(2-nitrobenzenesulfonyl)-1,4,7-triazaheptane **(7)** in DMSO-d_6 at 25°C.

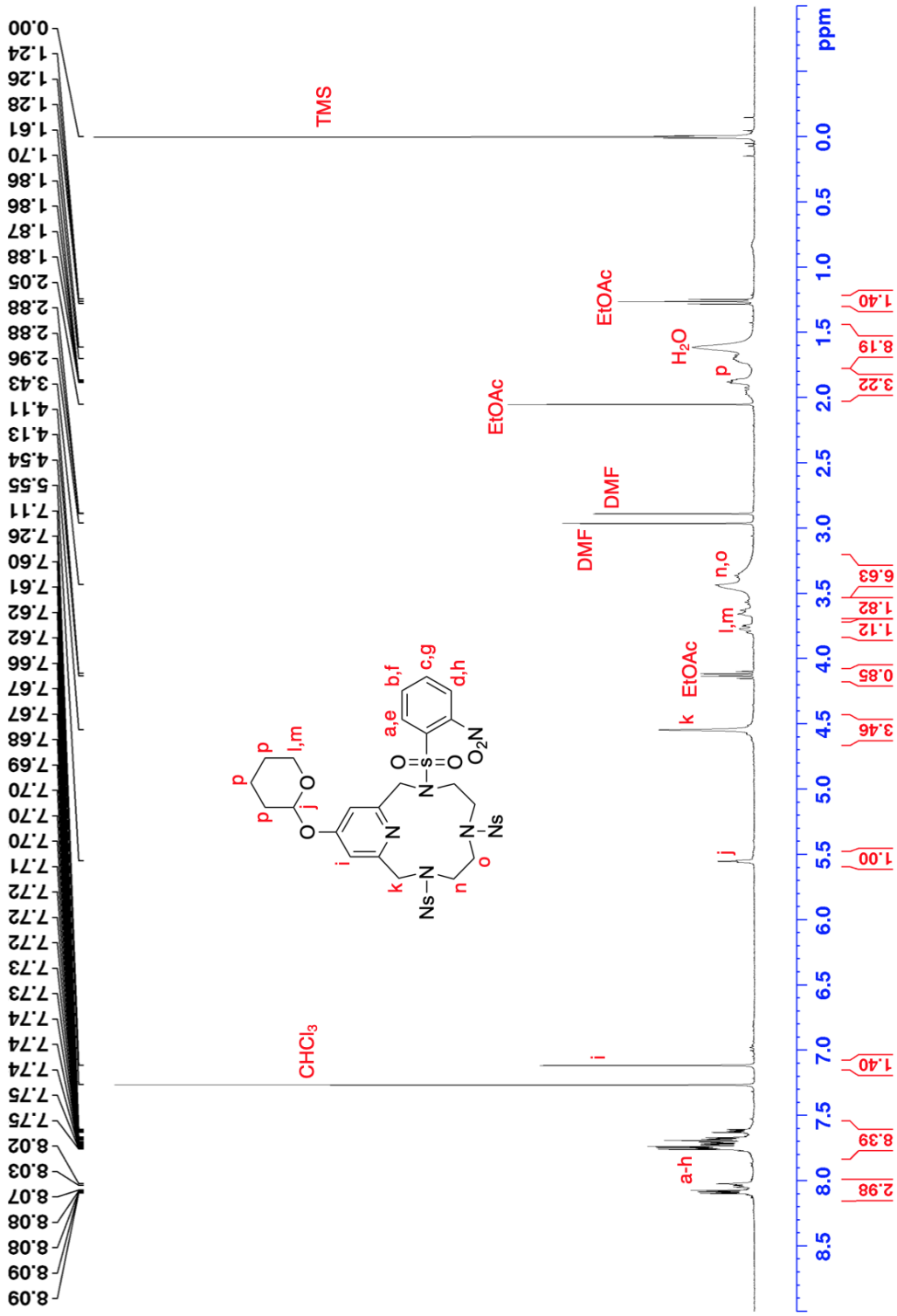

Figure S17: ^{1}H NMR of THP, Ns-protected ^{OH}**PyN$_3$ (8)** in $CDCl_3$ at 25°C.

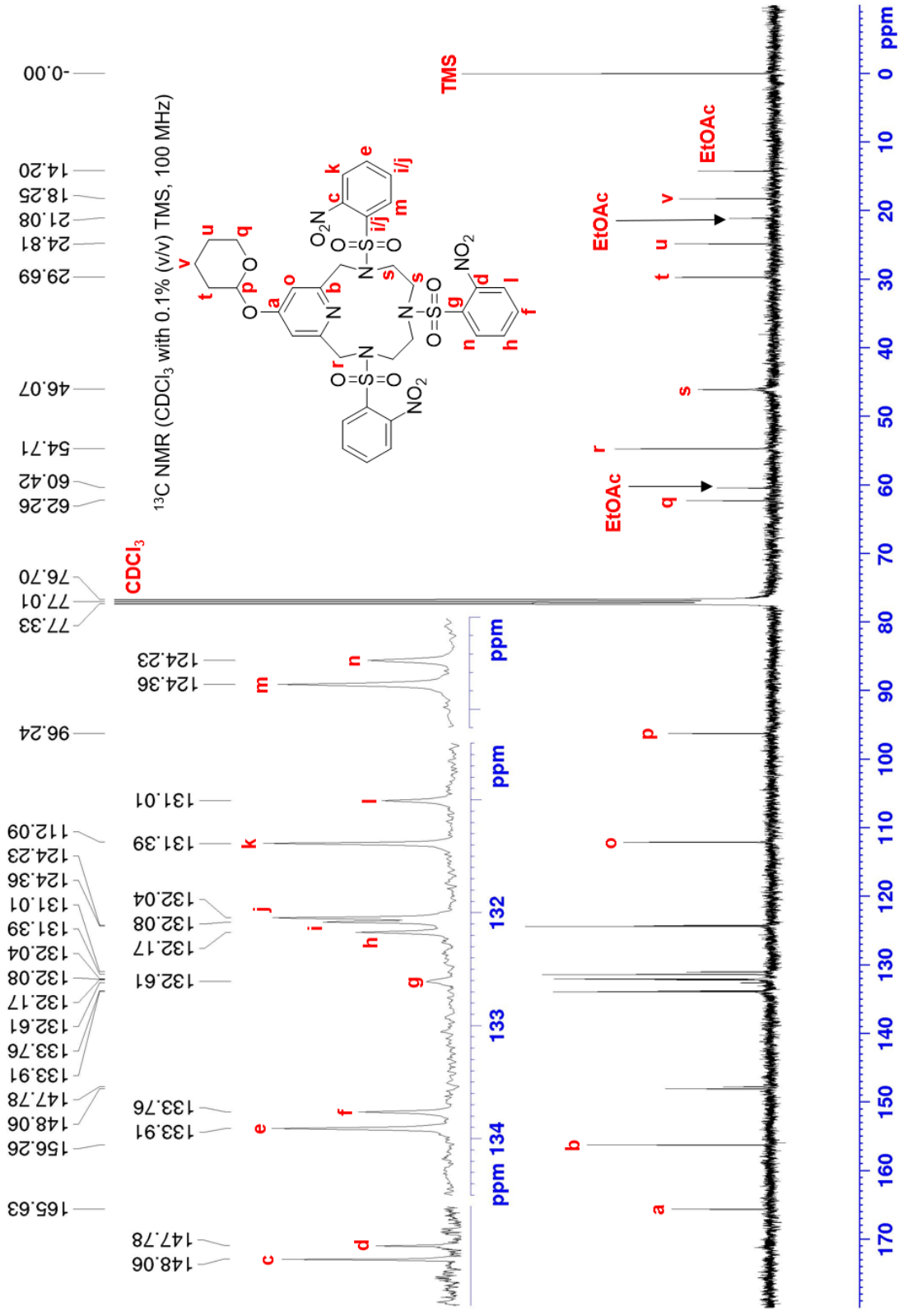

Figure S18: ^{13}C NMR of THP, Ns-protected ^{OH}**PyN$_3$ (8)** in $CDCl_3$ at 25°C.

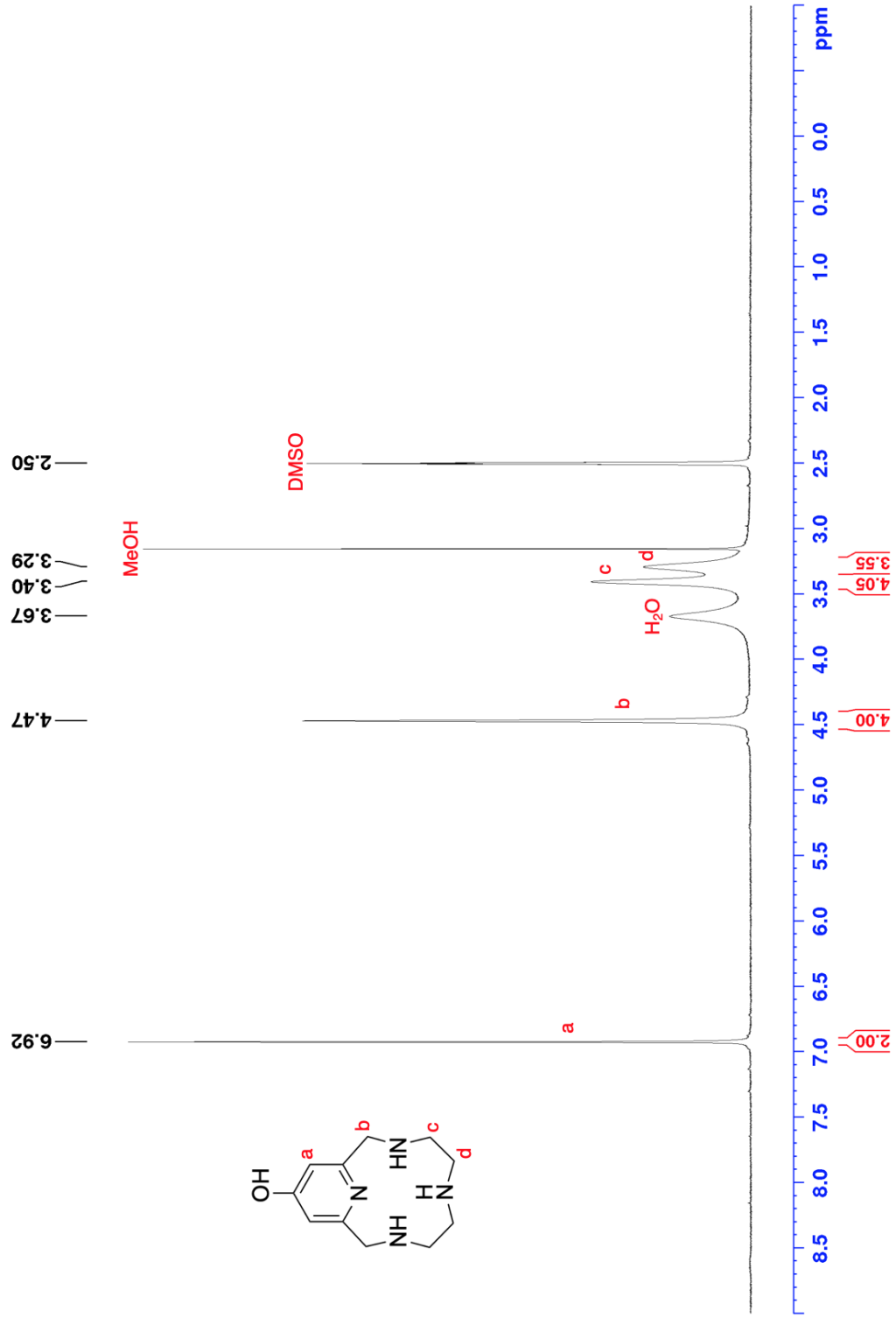

Figure S19: ^{1}H NMR of ^{OH}**PyN$_3$·HCl (9)** in DMSO at 25°C.

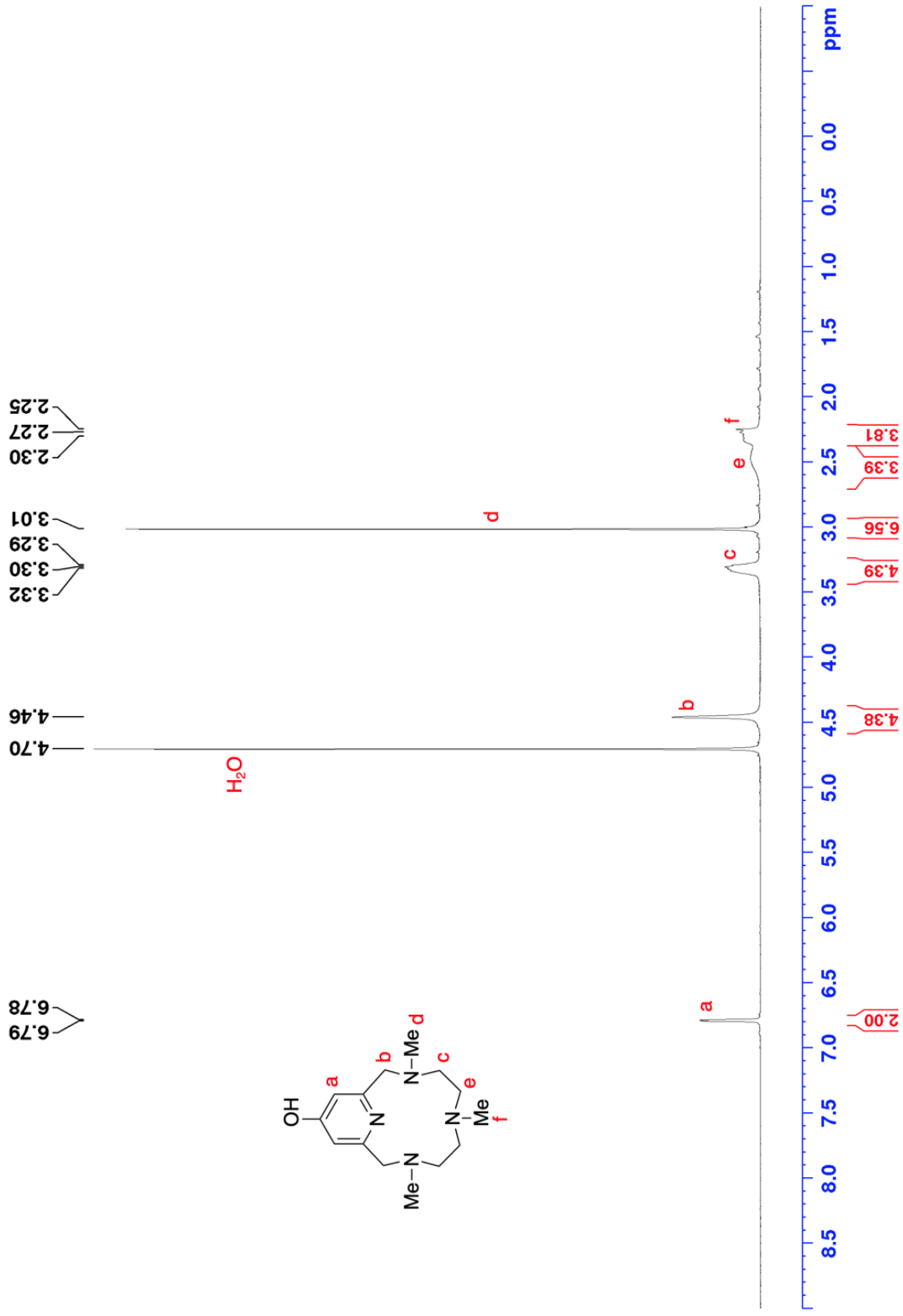

Figure S20: ^{1}H NMR of ^{OH}**PyNMe$_3$ (10)** in DMSO at 25°C.

References

1. Lincoln, K. M.; Gonzalez, P.; Richardson, T. E.; Julovich, D. A.; Saunders, R.; Simpkins, J. W.; Green, K. N., A potent antioxidant small molecule aimed at targeting metal-based oxidative stress in neurodegenerative disorders. *Chem Commun (Camb)* **2013,** *49* (26), 2712-2714.

2. Lincoln, K. M.; Offutt, M. E.; Hayden, T. D.; Saunders, R. E.; Green, K. N., Structural, Spectral, and Electrochemical Properties of Nickel(II), Copper(II), and Zinc(II) Complexes Containing 12-Membered Pyridine- and Pyridol-Based Tetra-aza Macrocycles. *Inorganic Chemistry* **2014,** *53* (3), 1406-1416.

3. Lincoln, K. M.; Richardson, T. E.; Rutter, L.; Gonzalez, P.; Simpkins, J. W.; Green, K. N., An N-heterocyclic amine chelate capable of antioxidant capacity and amyloid disaggregation. *ACS Chem Neurosci* **2012,** *3* (11), 919-927.

4. Lincoln, K. M.; Gonzalez, P.; Richardson, T. E.; Julovich, D. A.; Saunders, R.; Simpkins, J. W.; Green, K. N., A potent antioxidant small molecule aimed at targeting metal-based oxidative stress in neurodegenerative disorders. *Chemical Communications* **2013,** *49* (26), 2712-2714.

5. Green, K. N.; Johnston, H. M.; Burnett, M. E.; Brewer, S. M., Hybrid Antioxidant and Metal Sequestering Small Molecules Targeting the Molecular Features of Alzheimer's Disease. *Comments on Inorganic Chemistry* **2017,** *37* (3), 146-167.

6. Brewer, S. M.; Wilson, K. R.; Jones, D. G.; Reinheimer, E. W.; Archibald, S. J.; Prior, T. J.; Ayala, M. A.; Foster, A. L.; Hubin, T. J.; Green, K. N., Increase of Direct C–C Coupling Reaction Yield by Identifying Structural and Electronic Properties of High-Spin Iron Tetra-azamacrocyclic Complexes. *Inorganic Chemistry* **2018,** *57* (15), 8890-8902.

7. Green, K. N.; Pota, K.; Tircsó, G.; Gogolák, R. A.; Kinsinger, O.; Davda, C.; Blain, K.; Brewer, S. M.; Gonzalez, P.; Johnston, H. M.; Akkaraju, G., Dialing in on pharmacological features for a therapeutic antioxidant small molecule. *Dalton Trans* **2019,** *48* (33), 12430-12439.

8. Johnston, H. M.; Pota, K.; Barnett, M. M.; Kinsinger, O.; Braden, P.; Schwartz, T. M.; Hoffer, E.; Sadagopan, N.; Nguyen, N.; Yu, Y.; Gonzalez, P.; Tircsó, G.; Wu, H.; Akkaraju, G.; Chumley, M. J.; Green, K. N., Enhancement of the Antioxidant Activity and Neurotherapeutic Features through Pyridol Addition to Tetraazamacrocyclic Molecules. *Inorganic Chemistry* **2019,** *58* (24), 16771-16784.

9. Lin, J. H.; Lu, A. Y. H., Role of Pharmacokinetics and Metabolism in Drug Discovery and Development. *Pharmacological Reviews* **1997,** *49* (4), 403.

10. Smith, D. A. In *High-Throughput Screening — Brains Versus Brawn*, Pharmacokinetic Challenges in Drug Discovery, Berlin, Heidelberg, 2002//; Pelkonen, O.; Baumann, A.; Reichel, A., Eds. Springer Berlin Heidelberg: Berlin, Heidelberg, 2002; pp 203-212.

11. Venkatesh, S.; Lipper, R. A., Role of the development scientist in compound lead selection and optimization. *Journal of Pharmaceutical Sciences* **2000,** *89* (2), 145-154.

12. Esmieu, C.; Guettas, D.; Conte-Daban, A.; Sabater, L.; Faller, P.; Hureau, C., Copper-Targeting Approaches in Alzheimer's Disease: How To Improve the Fallouts Obtained from in Vitro Studies. *Inorganic Chemistry* **2019,** *58* (20), 13509-13527.

13. Di, L.; Kerns, E. H., Profiling drug-like properties in discovery research. *Current Opinion in Chemical Biology* **2003,** *7* (3), 402-408.

14. Pardridge, W. M., Blood–brain barrier delivery. *Drug Discovery Today* **2007,** *12* (1), 54-61.

15. Pajouhesh, H.; Lenz, G., Medicinal Chemical Properties of Successful Central Nervous System Drugs. *NeuroRx : the journal of the American Society for Experimental NeuroTherapeutics* **2005,** *2*, 541-53.

16. Gupta, S. P., QSAR studies on drugs acting at the central nervous system. *Chemical Reviews* **1989,** *89* (8), 1765-1800.

17. Kerns, E. H.; Di, L., Pharmaceutical profiling in drug discovery. *Drug Discovery Today* **2003,** *8* (7), 316-323.

18. Mantle, J. L.; Min, L.; Lee, K. H., Minimum Transendothelial Electrical Resistance Thresholds for the Study of Small and Large Molecule Drug Transport in a Human in Vitro Blood–Brain Barrier Model. *Molecular Pharmaceutics* **2016,** *13* (12), 4191-4198.

19. Pardridge, W. M., Transport of small molecules through the blood-brain barrier: biology and methodology. *Advanced Drug Delivery Reviews* **1995,** *15* (1), 5-36.

20. Lipinski, C. A., Lead- and drug-like compounds: the rule-of-five revolution. *Drug Discov Today Technol* **2004,** *1* (4), 337-41.

21. Lipinski, C. A.; Lombardo, F.; Dominy, B. W.; Feeney, P. J., Experimental and computational approaches to estimate solubility and permeability in drug discovery and development settings. *Adv Drug Deliv Rev* **2001,** *46* (1-3), 3-26.

22. Clark, D. E.; Pickett, S. D., Computational methods for the prediction of 'drug-likeness'. *Drug Discovery Today* **2000,** *5* (2), 49-58.

23. Kelder, J.; Grootenhuis, P. D. J.; Bayada, D. M.; Delbressine, L. P. C.; Ploemen, J.-P., Polar Molecular Surface as a Dominating Determinant for Oral Absorption and Brain Penetration of Drugs. *Pharmaceutical Research* **1999,** *16* (10), 1514-1519.

24. van de Waterbeemd, H.; Camenisch, G.; Folkers, G.; Chretien, J. R.; Raevsky, O. A., Estimation of blood-brain barrier crossing of drugs using molecular size and shape, and H-bonding descriptors. *J Drug Target* **1998,** *6* (2), 151-65.

25. Muehlbacher, M.; Spitzer, G. M.; Liedl, K. R.; Kornhuber, J., Qualitative prediction of blood–brain barrier permeability on a large and refined dataset. *Journal of Computer-Aided Molecular Design* **2011,** *25* (12), 1095-1106.

26. Liu, Y.; Kochi, A.; Pithadia, A. S.; Lee, S.; Nam, Y.; Beck, M. W.; He, X.; Lee, D.; Lim, M. H., Tuning Reactivity of Diphenylpropynone Derivatives with Metal-Associated Amyloid-β Species via Structural Modifications. *Inorganic Chemistry* **2013,** *52* (14), 8121-8130.

27. Lee, S.; Zheng, X.; Krishnamoorthy, J.; Savelieff, M. G.; Park, H. M.; Brender, J. R.; Kim, J. H.; Derrick, J. S.; Kochi, A.; Lee, H. J.; Kim, C.; Ramamoorthy, A.; Bowers, M. T.; Lim, M. H., Rational Design of a Structural Framework with Potential Use to Develop Chemical Reagents That Target and Modulate Multiple Facets of Alzheimer's Disease. *Journal of the American Chemical Society* **2014,** *136* (1), 299-310.

28. Nguyen, L. N.; Ma, D.; Shui, G.; Wong, P.; Cazenave-Gassiot, A.; Zhang, X.; Wenk, M. R.; Goh, E. L.; Silver, D. L., Mfsd2a is a transporter for the essential omega-3 fatty acid docosahexaenoic acid. *Nature* **2014,** *509* (7501), 503-6.

29. Wellhauser, L.; Belsham, D. D., Activation of the omega-3 fatty acid receptor GPR120 mediates anti-inflammatory actions in immortalized hypothalamic neurons. *Journal of Neuroinflammation* **2014,** *11* (1), 60.

30. Calder, P. C., Omega-3 fatty acids and inflammatory processes. *Nutrients* **2010,** *2* (3), 355-374.

31. Simopoulos, A. P., Omega-3 fatty acids in inflammation and autoimmune diseases. *J Am Coll Nutr* **2002,** *21* (6), 495-505.

32. Avdeef, A.; Bendels, S.; Di, L. i.; Faller, B.; Kansy, M.; Sugano, K.; Yamauchi, Y., PAMPA—critical factors for better predictions of absorption. *Journal of Pharmaceutical Sciences* **2007,** *96* (11), 2893-2909.

33. Nikac, M.; Brimble, M. A.; Crumbie, R. L., Synthesis of thiacrown and azacrown ethers based on a spiroacetal framework. *Tetrahedron* **2007,** *63* (24), 5220-5226.

34. Lin, H.; Long, J. Z.; Roche, A. M.; Svensson, K. J.; Dou, F. Y.; Chang, M. R.; Strutzenberg, T.; Ruiz, C.; Cameron, M. D.; Novick, S. J.; Berdan, C. A.; Louie, S. M.; Nomura, D. K.; Spiegelman, B. M.; Griffin, P. R.; Kamenecka, T. M., Discovery of Hydrolysis-Resistant Isoindoline N-Acyl Amino Acid Analogues that Stimulate Mitochondrial Respiration. *Journal of Medicinal Chemistry* **2018,** *61* (7), 3224-3230.